Electronic Supplementary Information

Catecholase activity of Mannich-based dinuclear Cu^{II} complexes with theoretical modeling: New insight into the solvent role in catalytic cycle†

Ria Sanyal,[a] Priyanka Kundu,[a] Elena Rychagova,[b,c] Grigory Zhigulin,[b] Sergey Ketkov,[b,c] Bipinbihari Ghosh,[d] Shyamal Kumar Chattopadhyay,[d] Ennio Zangrando*[,e] and Debasis Das*[a]

[a]*Department of Chemistry, University of Calcutta, 92, A. P. C. Road, Kolkata – 700009, India. Fax: +913323519755; Tel: +913324837031; E-mail: dasdebasis2001@yahoo.com.*

[b]*G.A.Razuvaev Institute of Organometallic Chemistry RAS, 49 Tropinin St., 603950 Nizhny Novgorod, Russian Federation.*

[c]*N. I. Lobachevsky Nizhny Novgorod State University, Gagarin ave. 23, 603950 Nizhny Novgorod, Russian Federation.*

[d]*Department of Chemistry, Indian Institute of Engineering Science and Technology, Howrah 711103, India.*

[e]*Department of Chemical and Pharmaceutical Sciences, University of Trieste, Via L. Giorgieri 1, 34127 Trieste, Italy. E-mail: zangrando@units.it.*

Table of contents

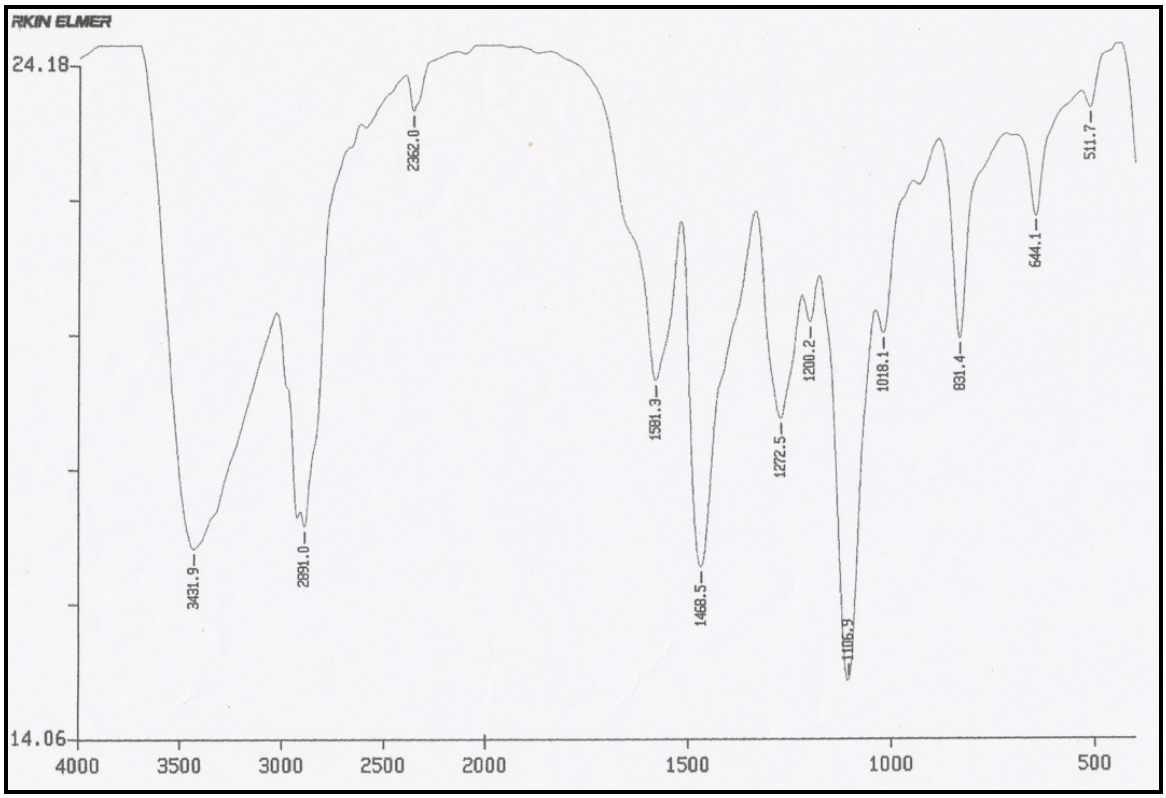

Fig. S1 FTIR spectra of ligand **HL1** in NaCl-plate.

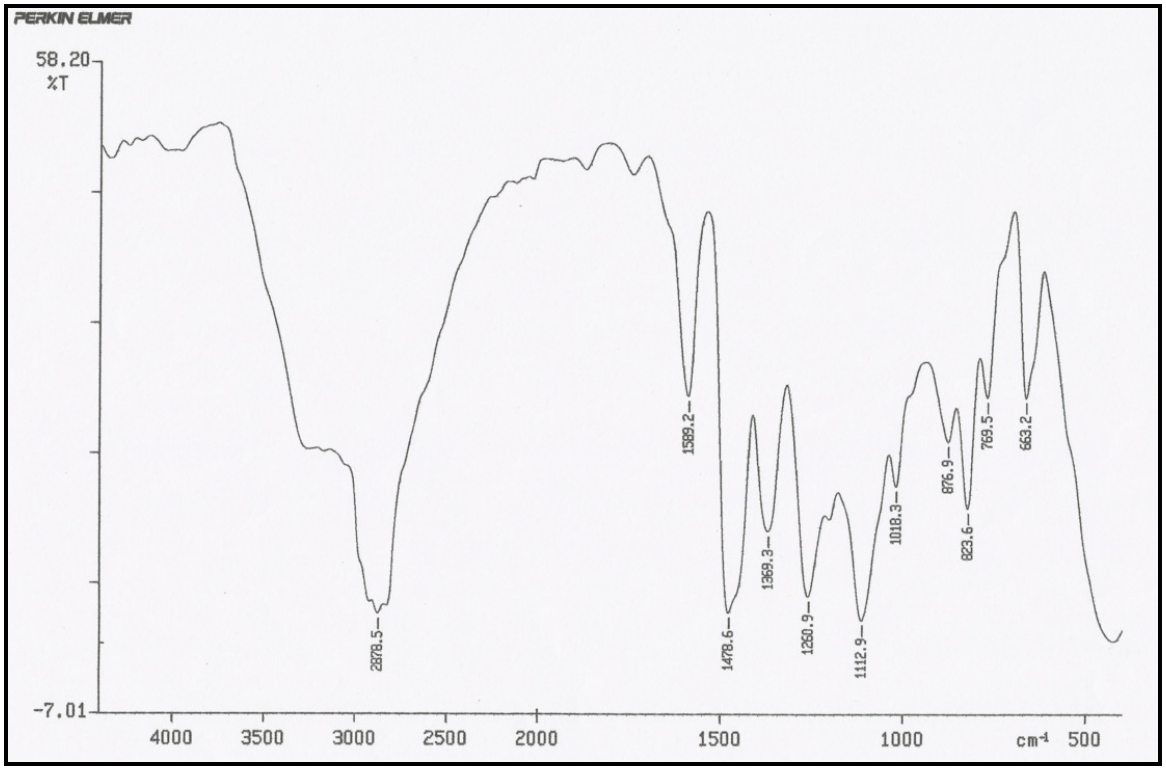

Fig. S2 FTIR spectra of ligand **HL2** in NaCl-plate.

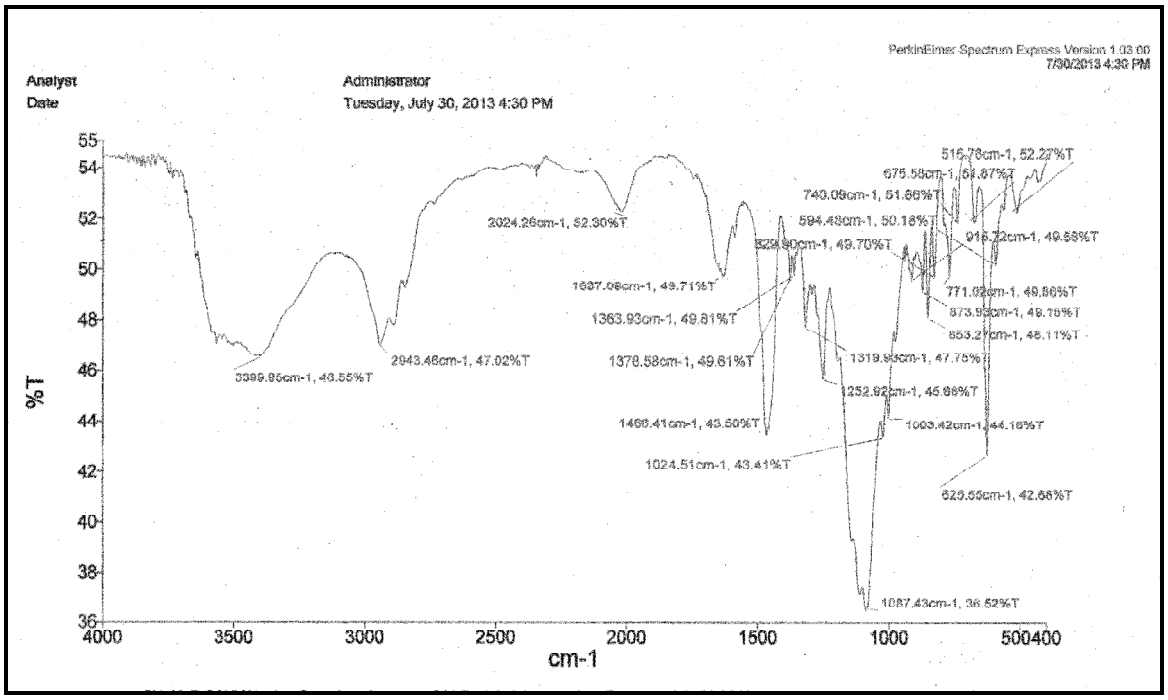

Fig. S3 FTIR spectrum of complex **1** in KBr pellet.

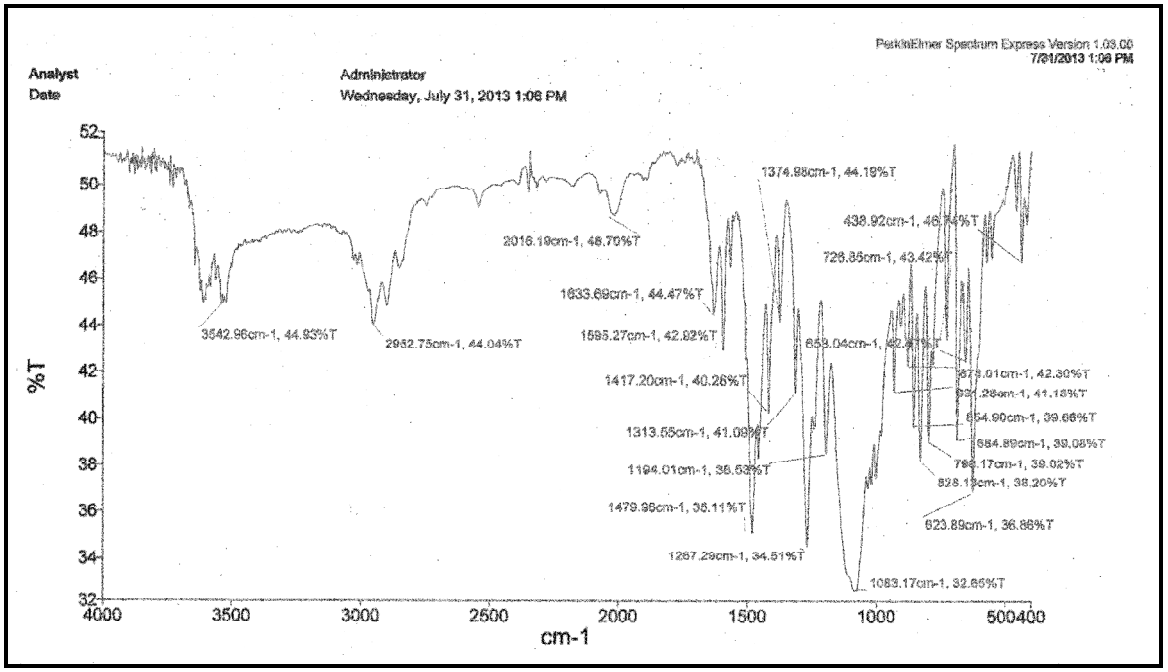

Fig. S4 FTIR spectrum of complex **2** in KBr pellet.

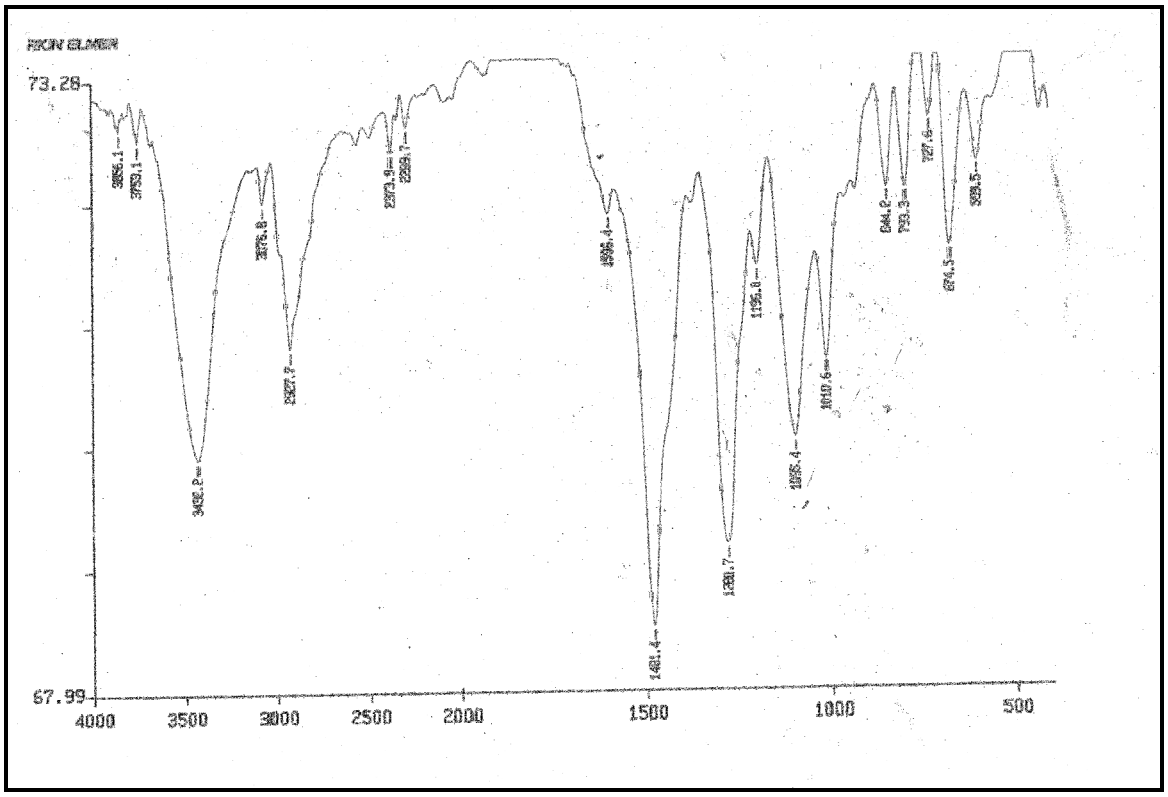

Fig. S5 FTIR spectrum of complex **3** in KBr pellet.

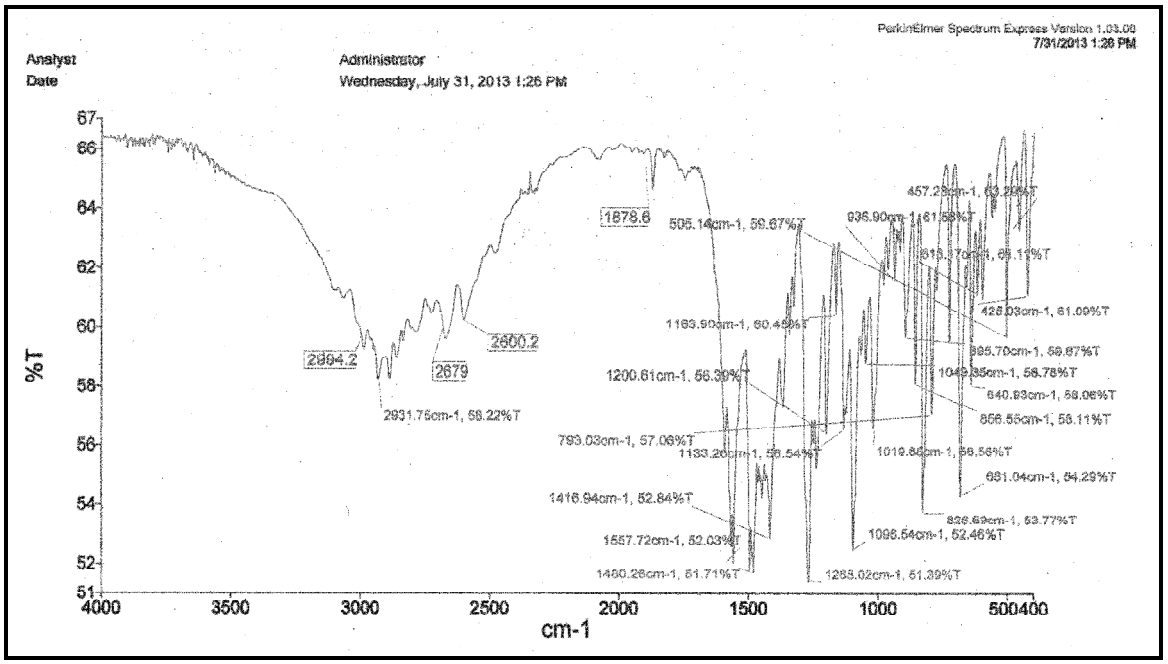

Fig. S6 FTIR spectrum of complex **4** in KBr pellet.

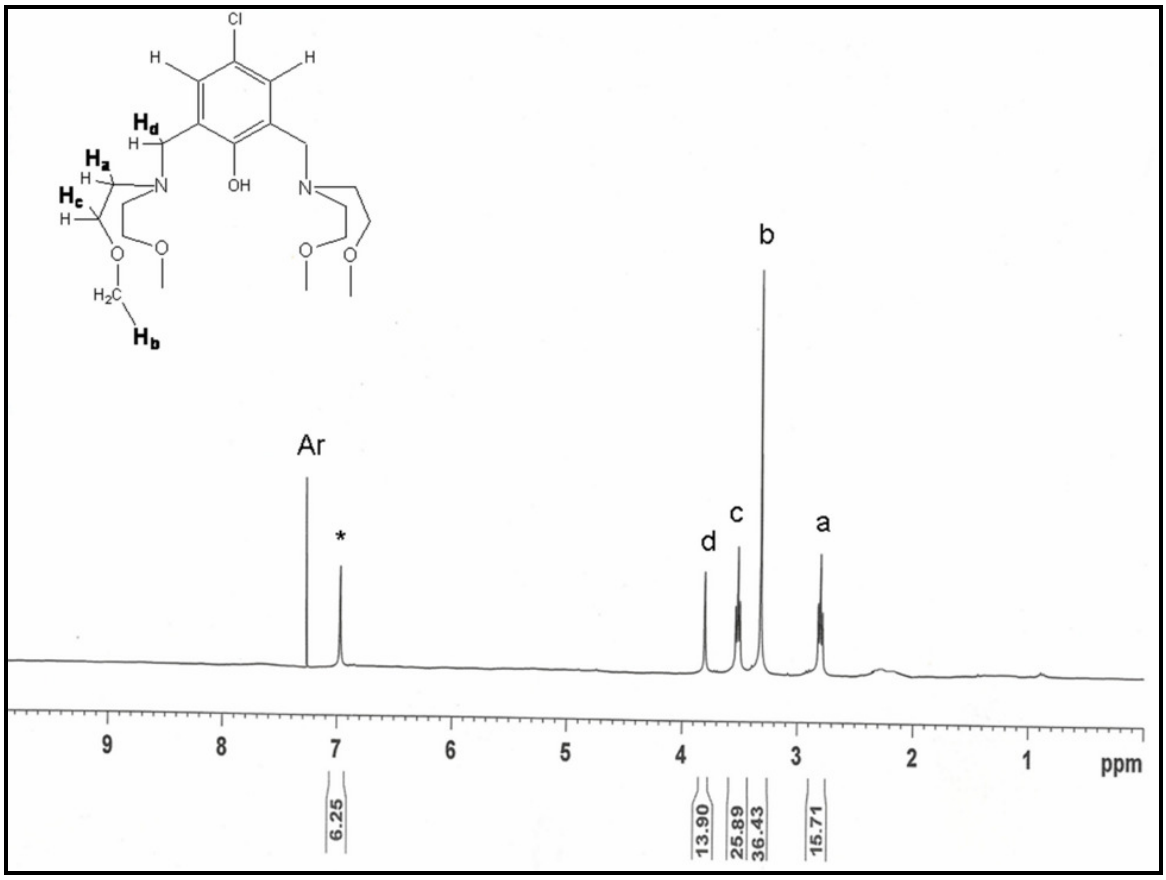

Fig. S7 ^{1}H-NMR of ligand **HL1** in $CDCl_3$ at 25°C (Solvent peak is marked as *).

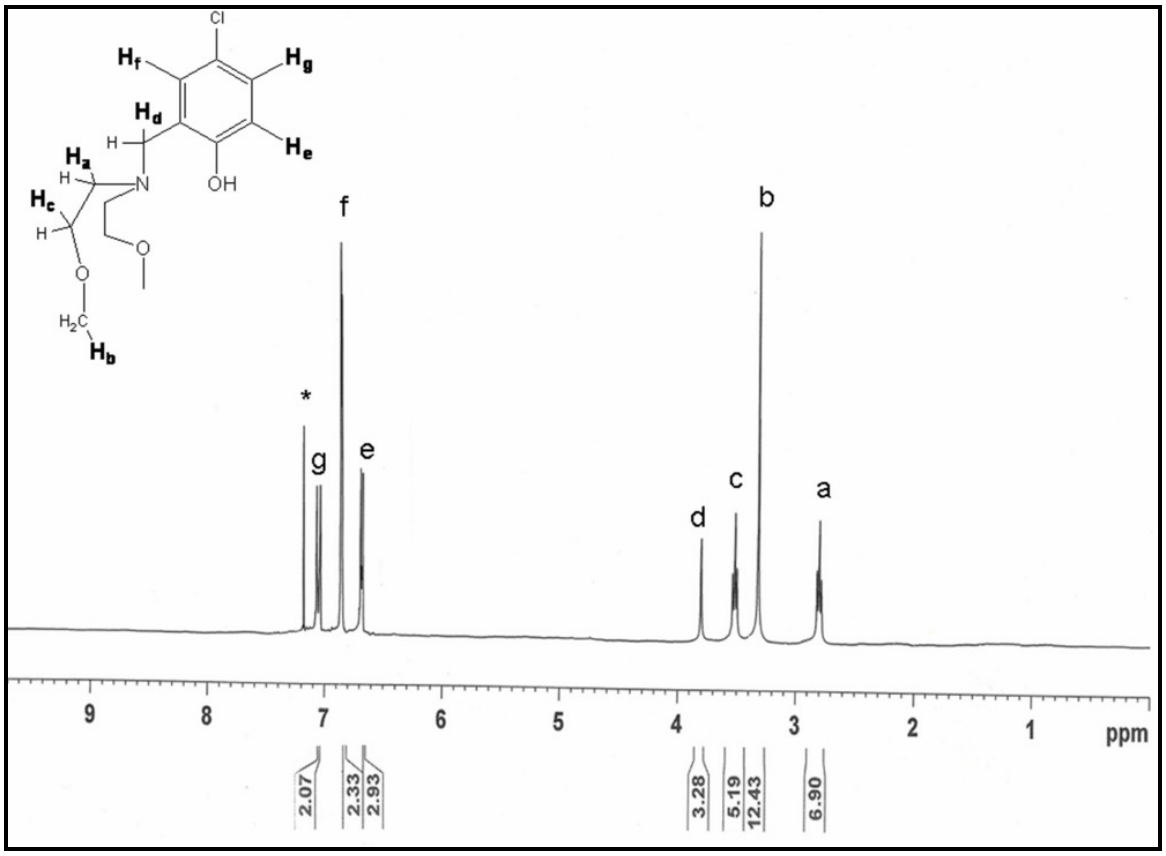

Fig. S8 ^{1}H-NMR of ligand **HL2** in $CDCl_3$ at 25°C (Solvent peak is marked as *).

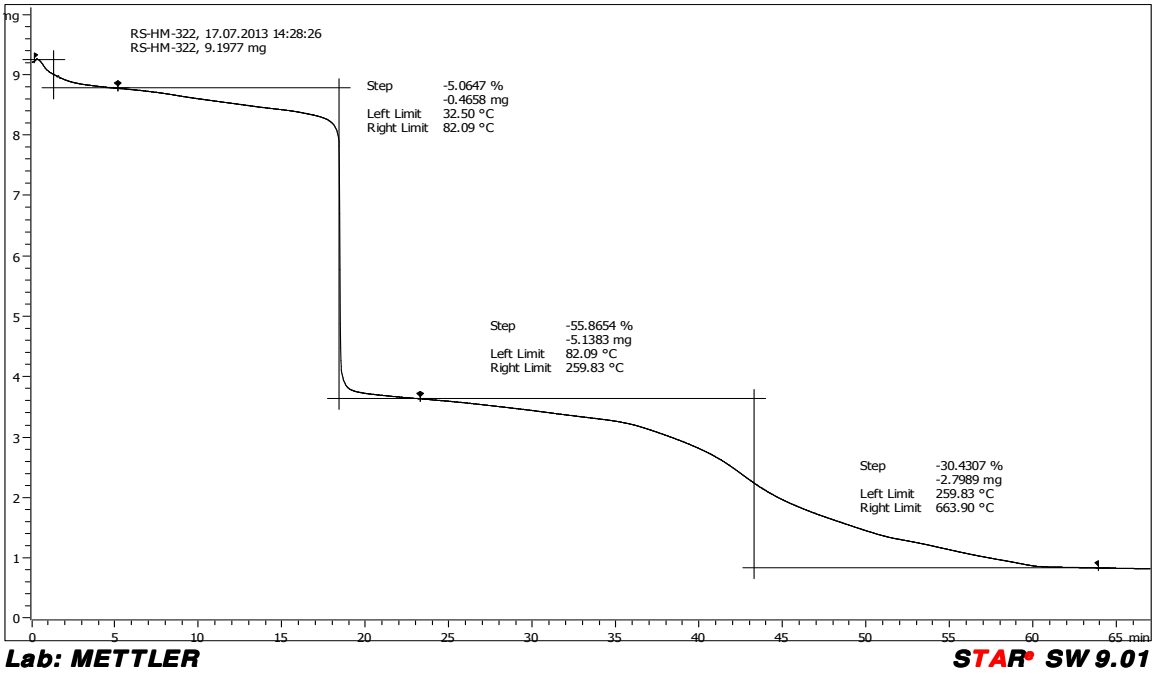

Fig. S9 TGA curve of complex **3**.

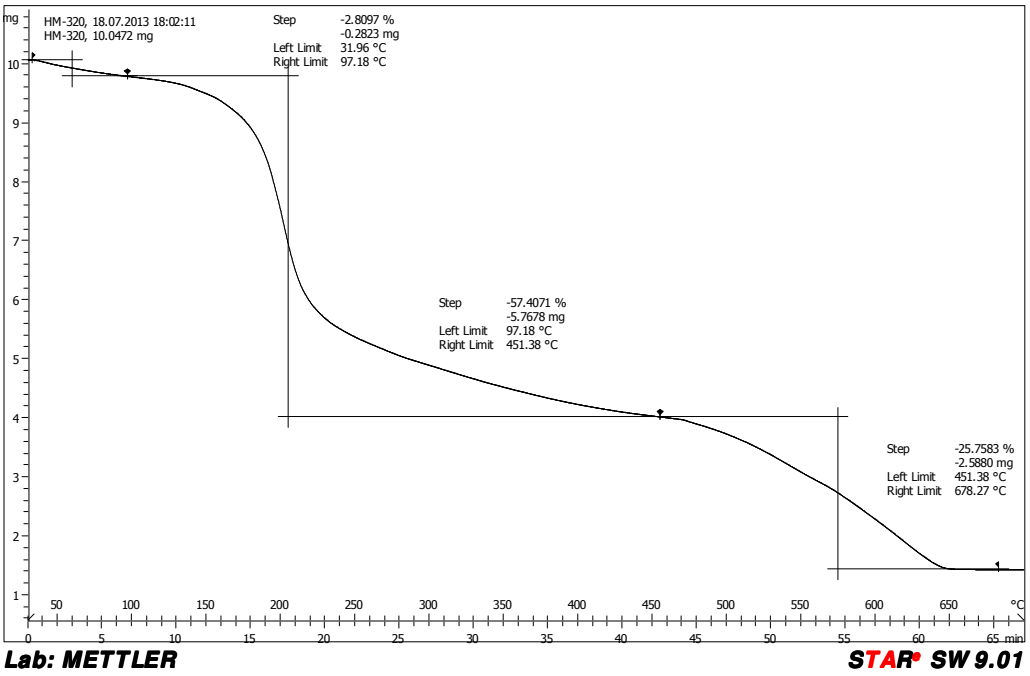

Fig. S10 TGA curve of complex **4**.

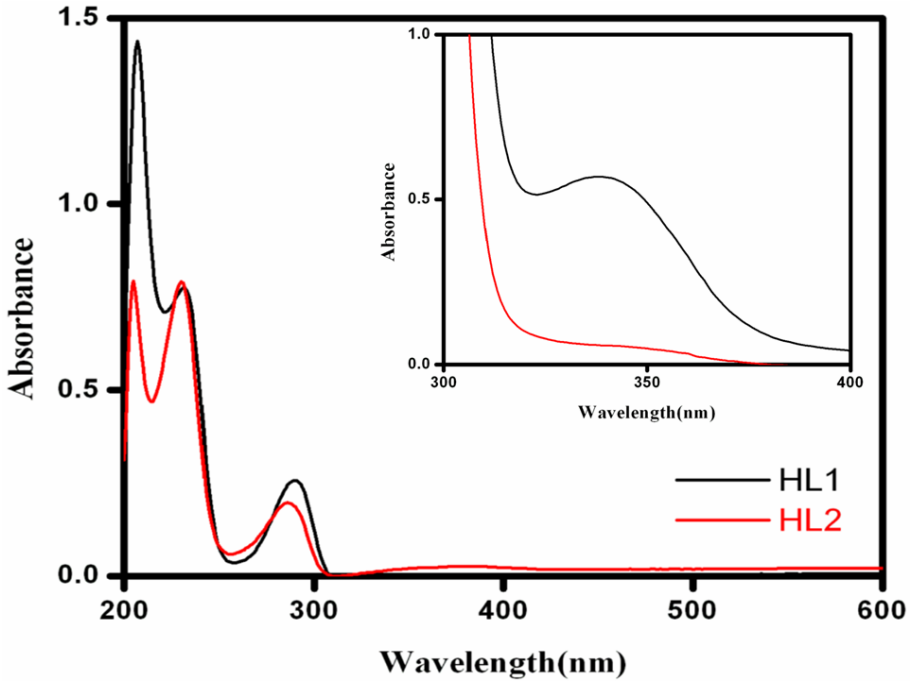

Fig. S11 Electronic spectra of the free ligands in acetonitrile at 25°C.

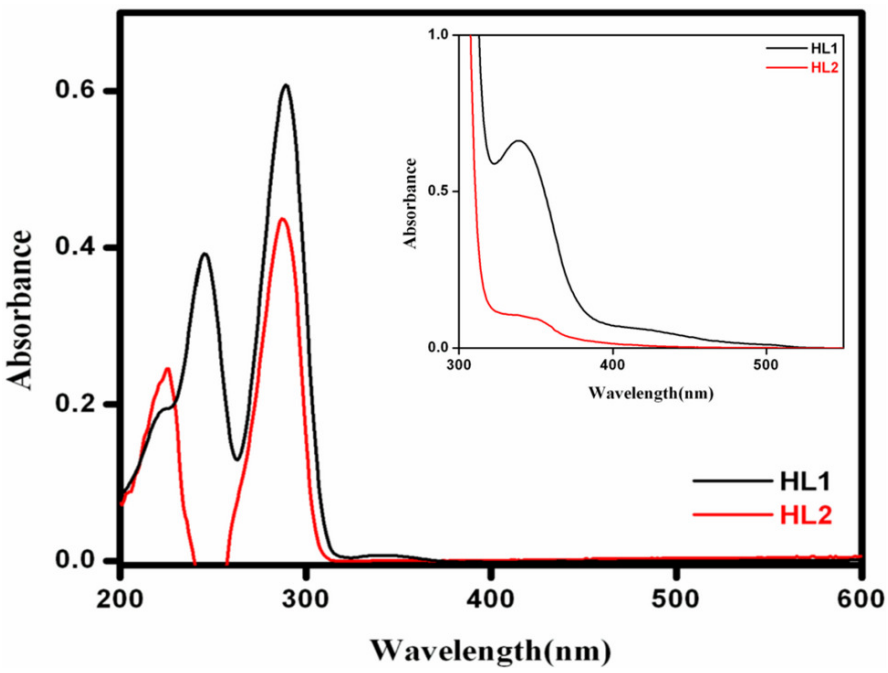

Fig. S12 Electronic spectra of the free ligands in DMSO at 25°C.

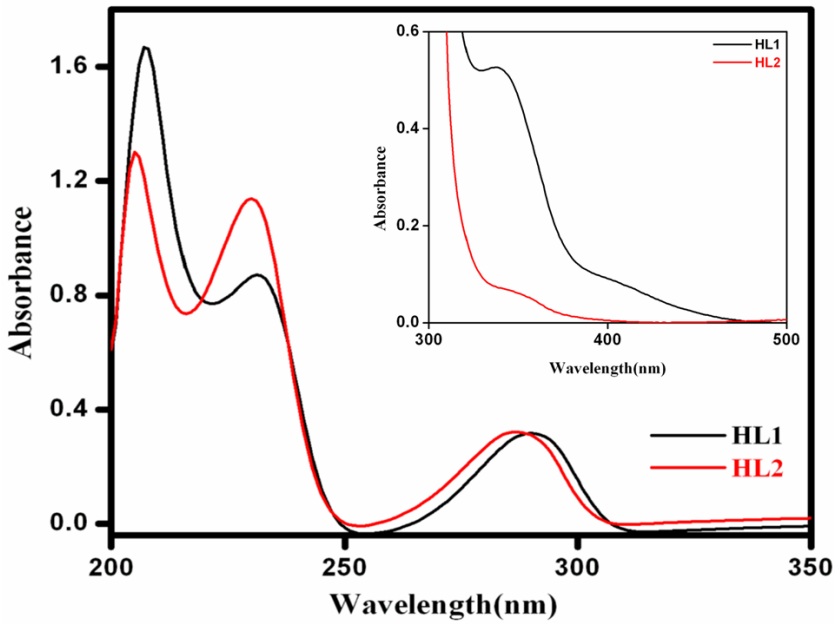

Fig. S13 Electronic spectra of the free ligands in methanol at 25°C.

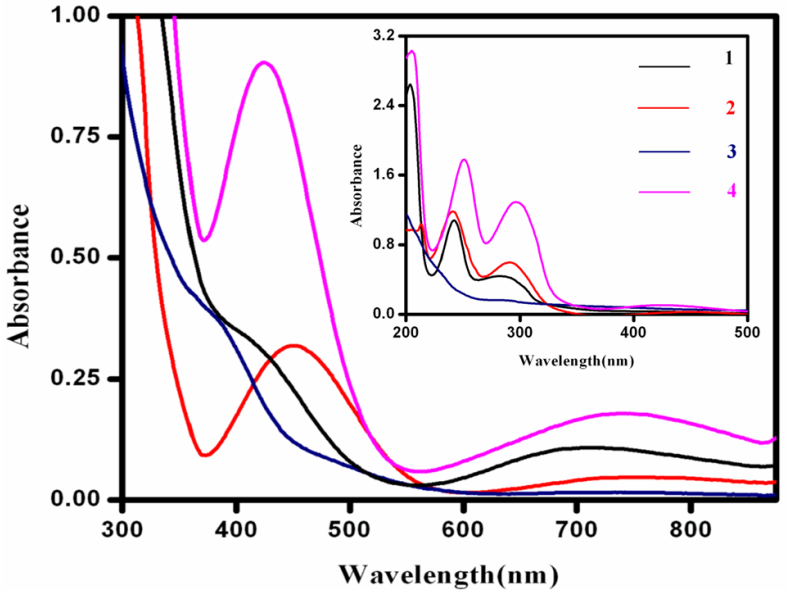

Fig. S14 Electronic spectra of 10^{-3} M acetonitrile solution of complexes **1**-**4** and in the inset of 10^{-4} M solution.

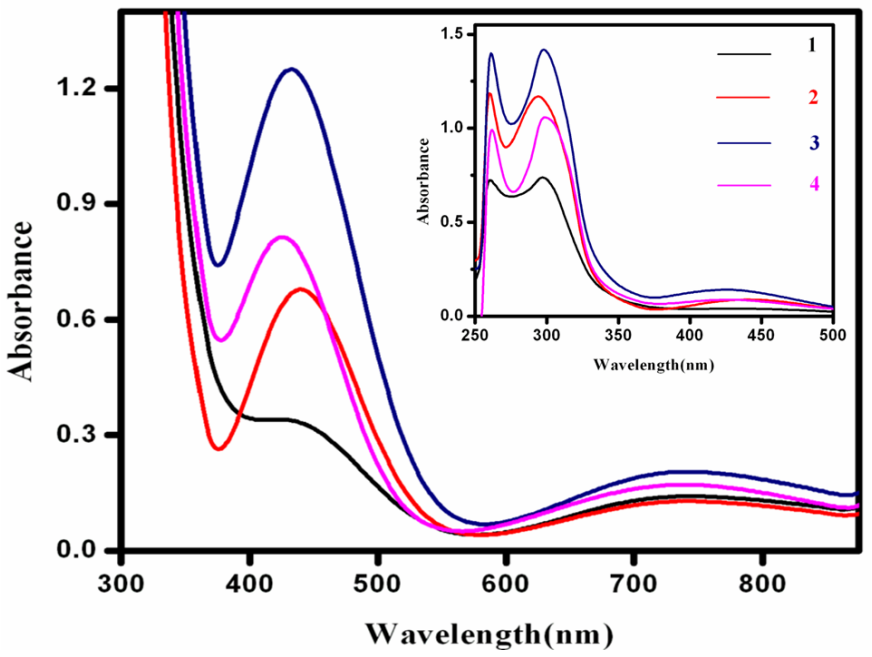

Fig. S15 Electronic spectra of 10^{-3} M DMSO solution of complexes **1**-**4** and in the inset of 10^{-4} M solution.

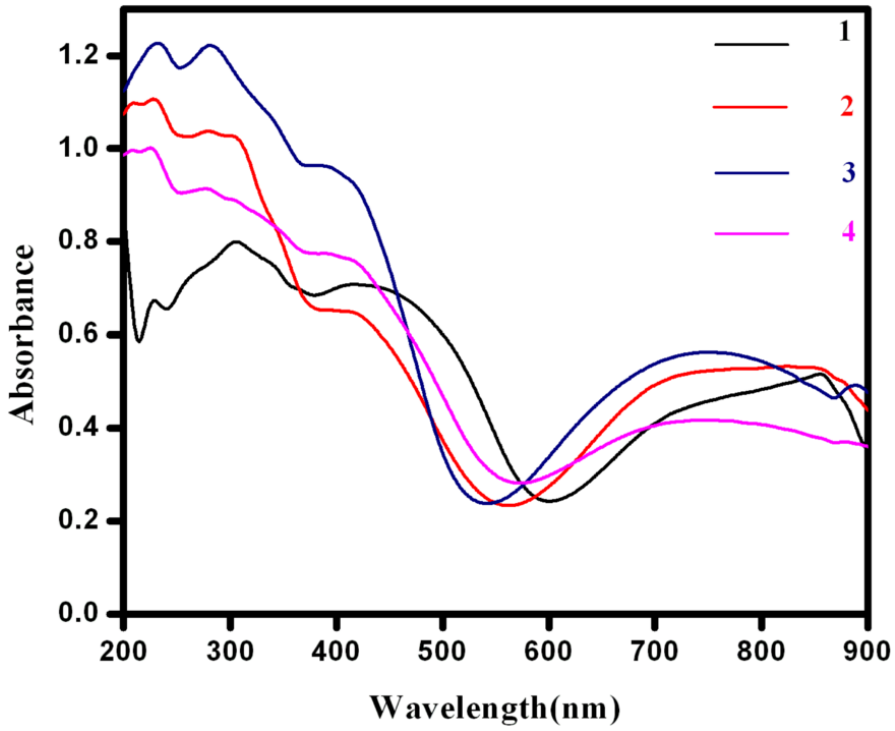

Fig. S16 Electronic spectra of complex **1-4** in the solid-state at 25°C.

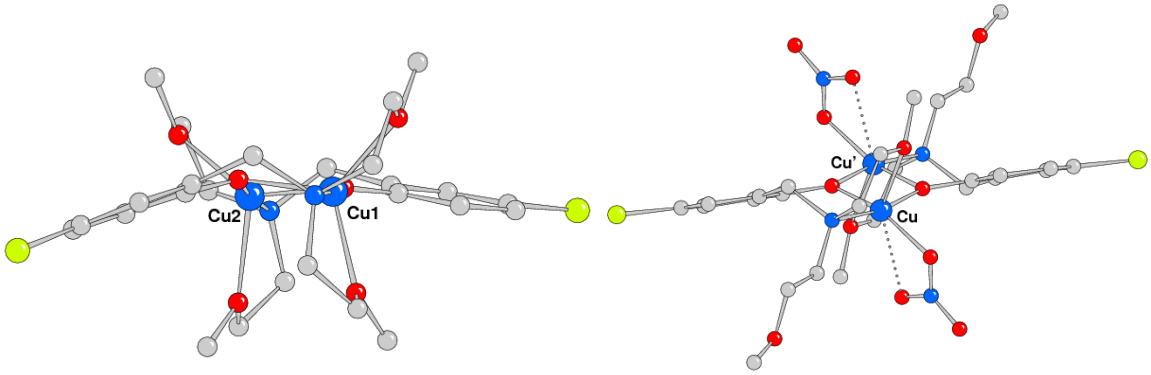

Fig. S17 Side view of complexes **3** and **4** showing the different orientation of the phenolato moieties. Complex **4** shows a comparable arranegement of **3**, substituting the nitrates with acetate anions.

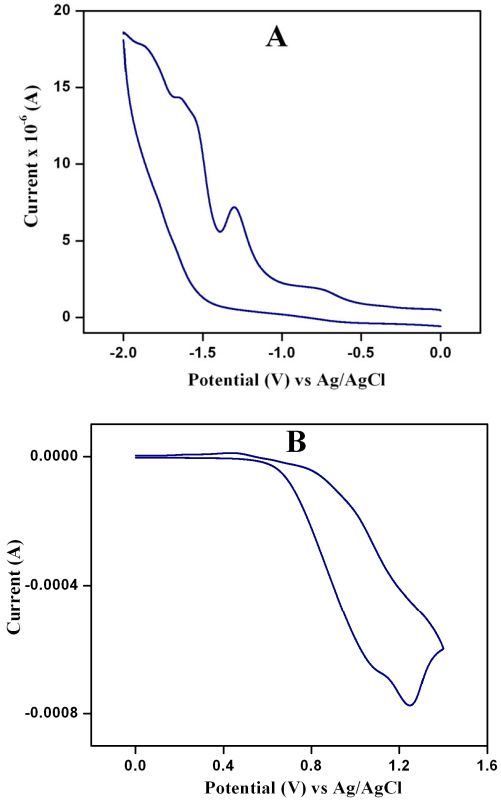

Fig. S18 Cyclic voltammograms of ligand **HL1** in acetonitrile representing (A) reductive wave and (B) oxidative wave.

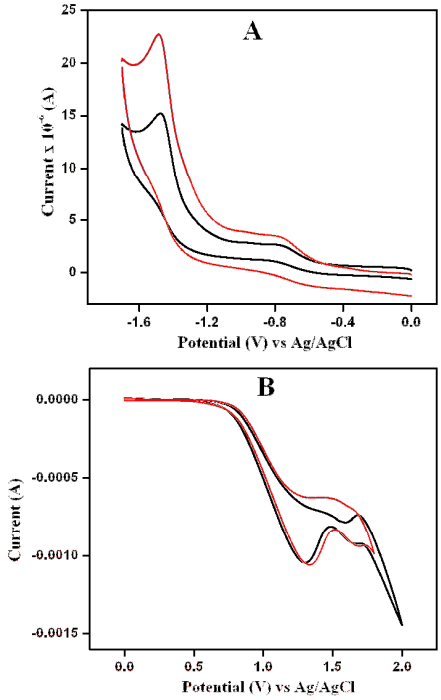

Fig. S19 Cyclic voltammograms of ligand **HL2** in acetonitrile representing (A) reductive wave and (B) oxidative wave.

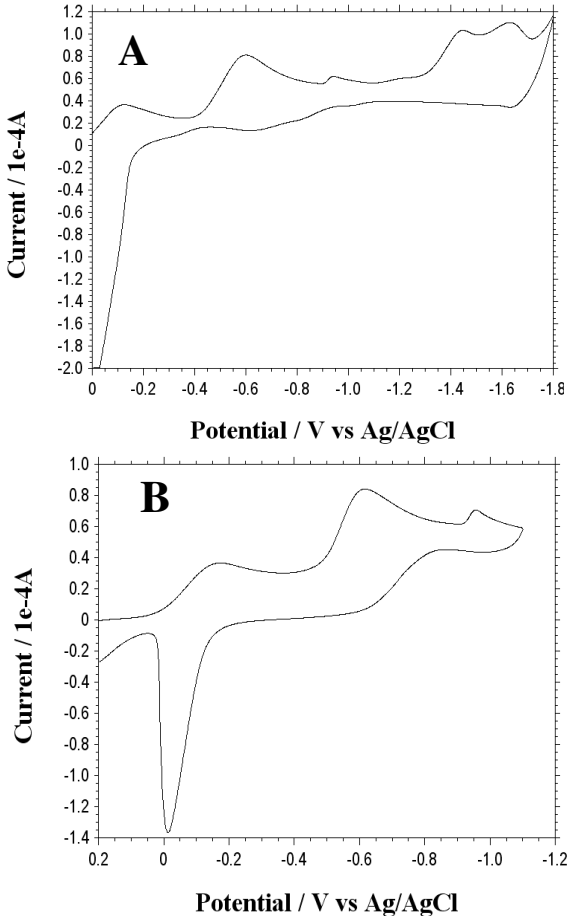

Fig. S20 Cyclic voltammogram of complex **1** (10^{-3} M) in acetonitrile.

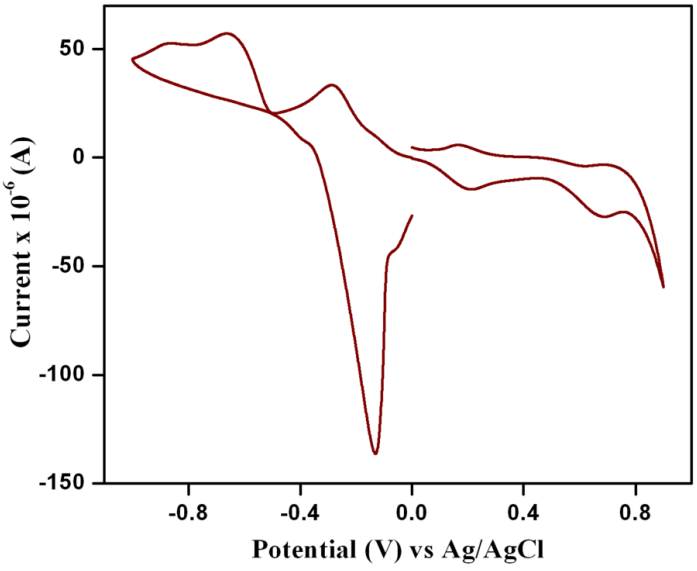

Fig. S21 Cyclic voltammogram of a mixture of complex **1** and 3,5-DTBC (1:100) in acetonitrile.

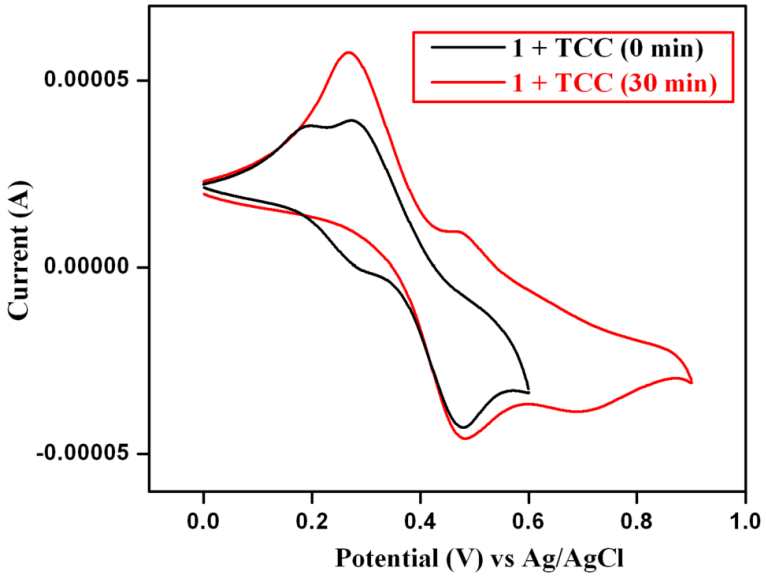

Fig. S22 Cyclic voltammogram of a mixture of complex **1** and TCC (1:100) in acetonitrile.

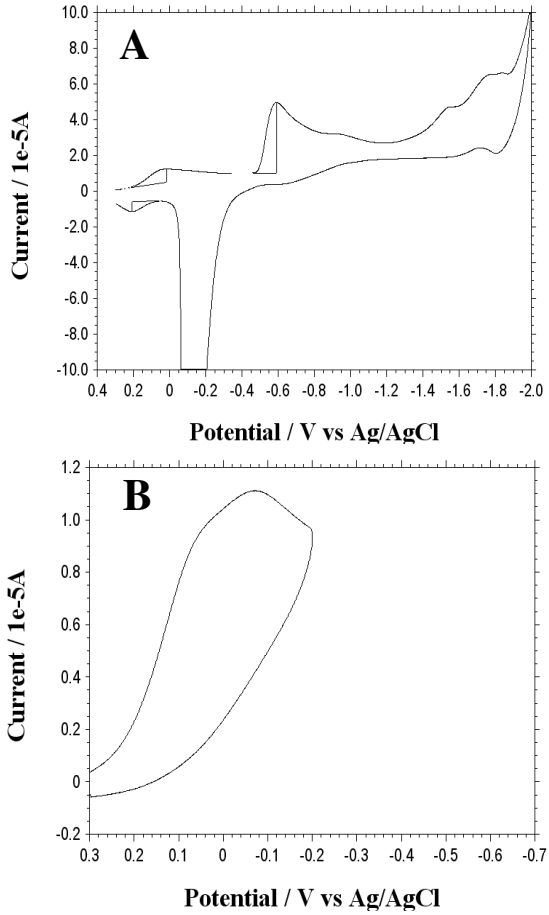

Fig. S23 Cyclic voltammogram of complex **2** (10^{-3} M) in acetonitrile.

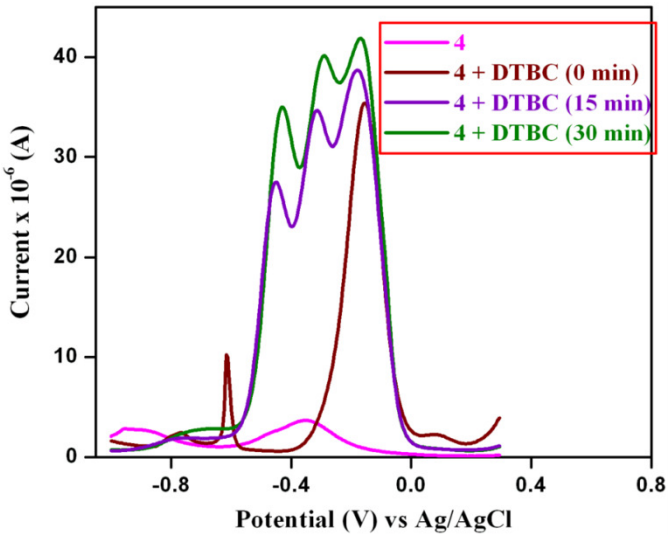

Fig. S24 Differential pulse voltammogram of complex **4** in absence and presence of 3,5-DTBC in acetonitrile.

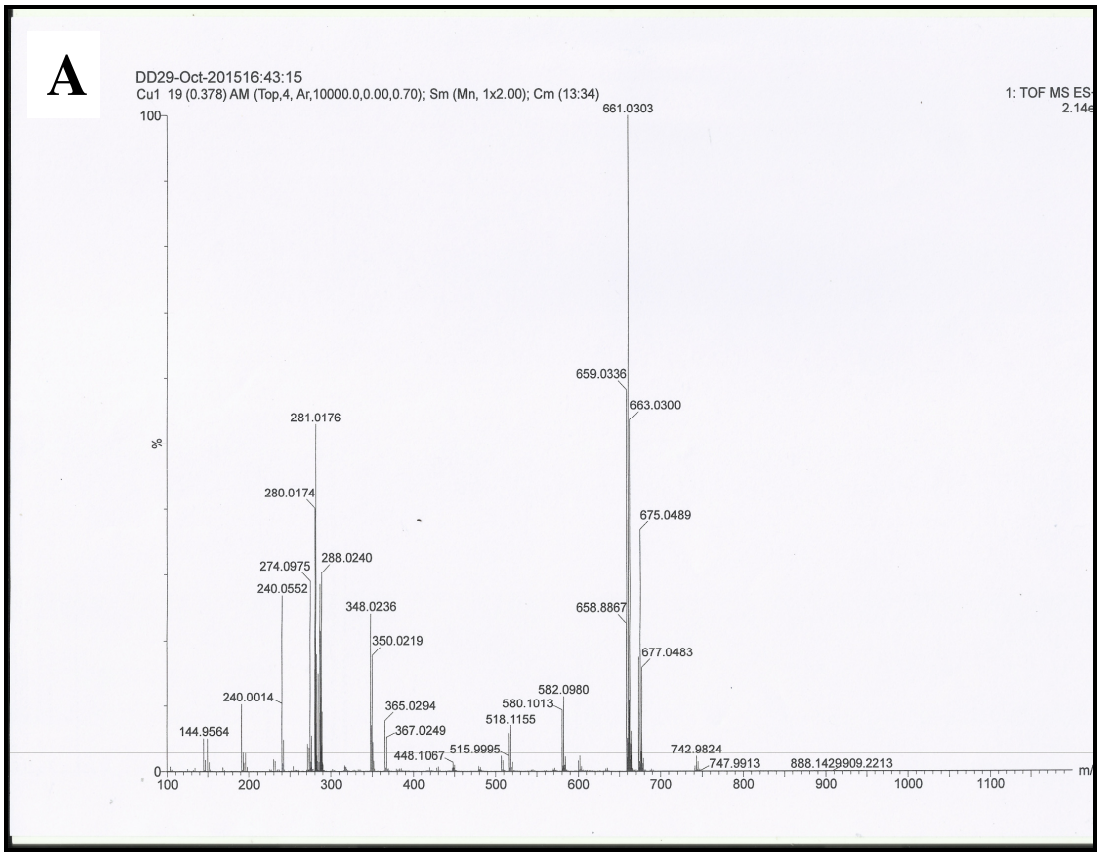
A
DD29-Oct-201516:43:15
Cu1 19 (0.378) AM (Top,4, Ar,10000.0,0.00,0.70); Sm (Mn, 1x2.00); Cm (13:34)
1: TOF MS ES
2.14e
661.0303
659.0336
663.0300
281.0176
280.0174
675.0489
288.0240
274.0975
240.0552
348.0236
658.8867
350.0219
677.0483
582.0980
240.0014
365.0294
580.1013
518.1155
144.9564
367.0249
448.1067
515.9995
742.9824
747.9913
888.1429909.2213
%
m/
100
200
300
400
500
600
700
800
900
1000
1100

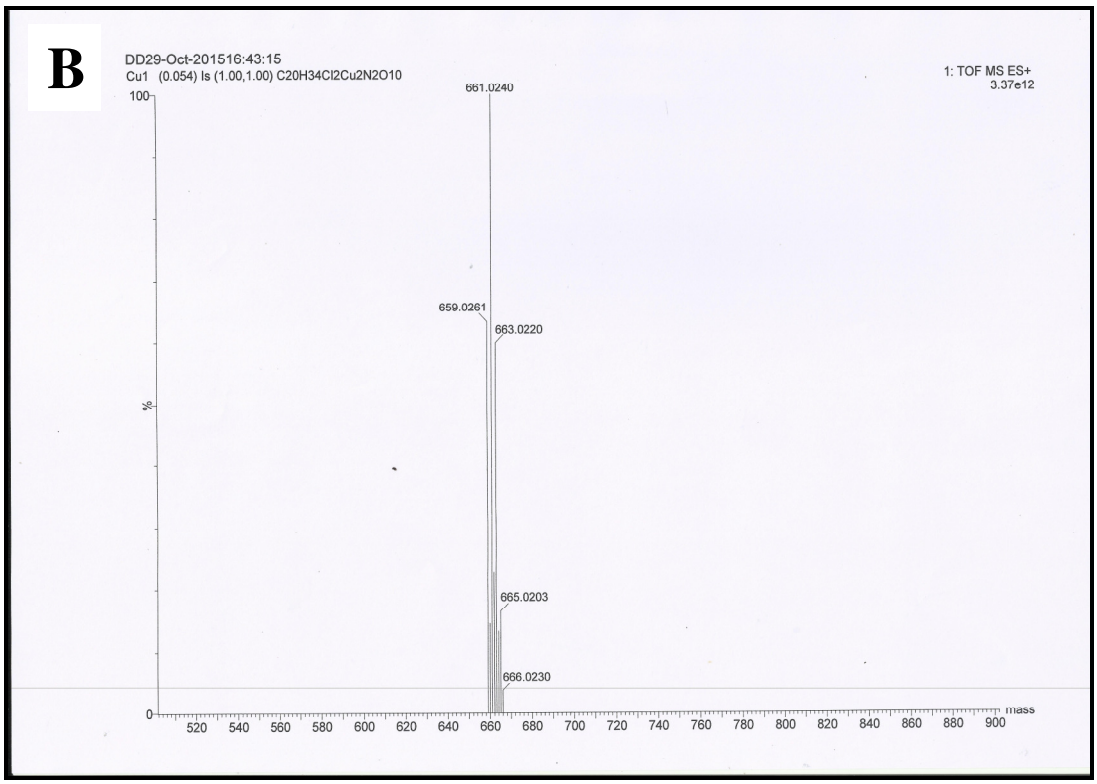
B
DD29-Oct-201516:43:15
Cu1 (0.054) Is (1.00,1.00) C20H34Cl2Cu2N2O10
1: TOF MS ES+
3.37e12
661.0240
659.0261
663.0220
665.0203
666.0230
%
mass
520
540
560
580
600
620
640
660
680
700
720
740
760
780
800
820
840
860
880
900

Fig. S25 ESI-MS spectrum of complex **1** in acetonitrile **(A)** experimental **(B)** simulated.

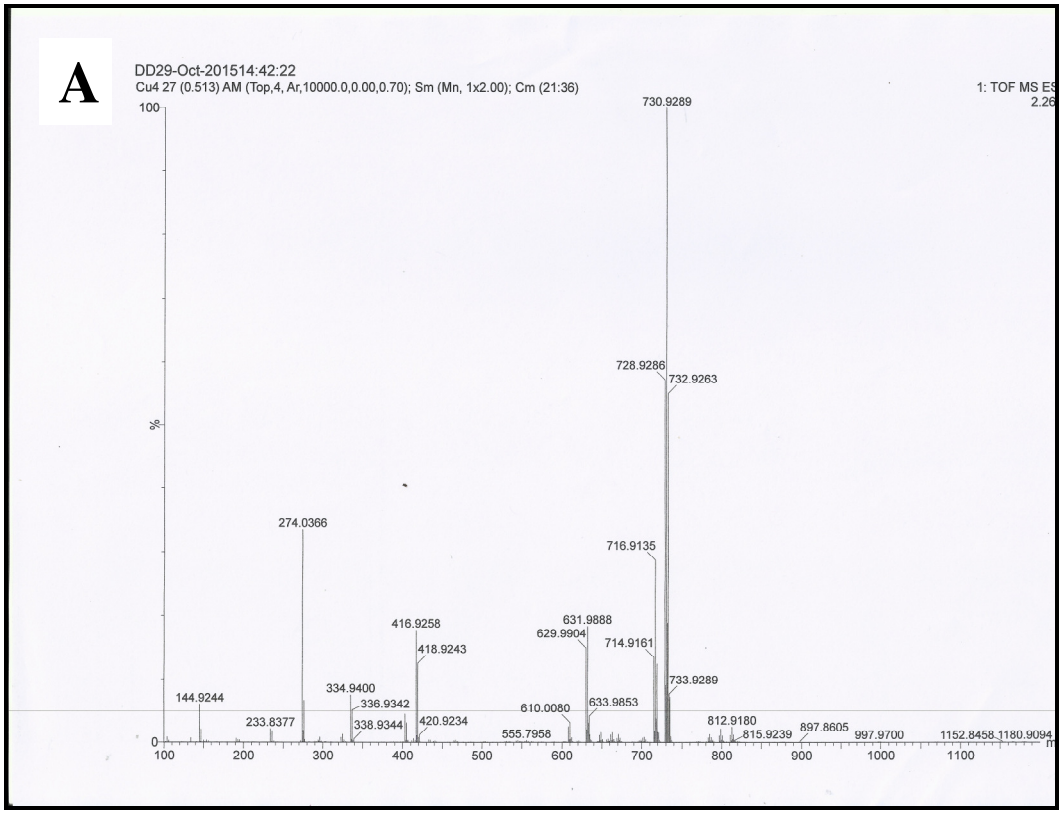

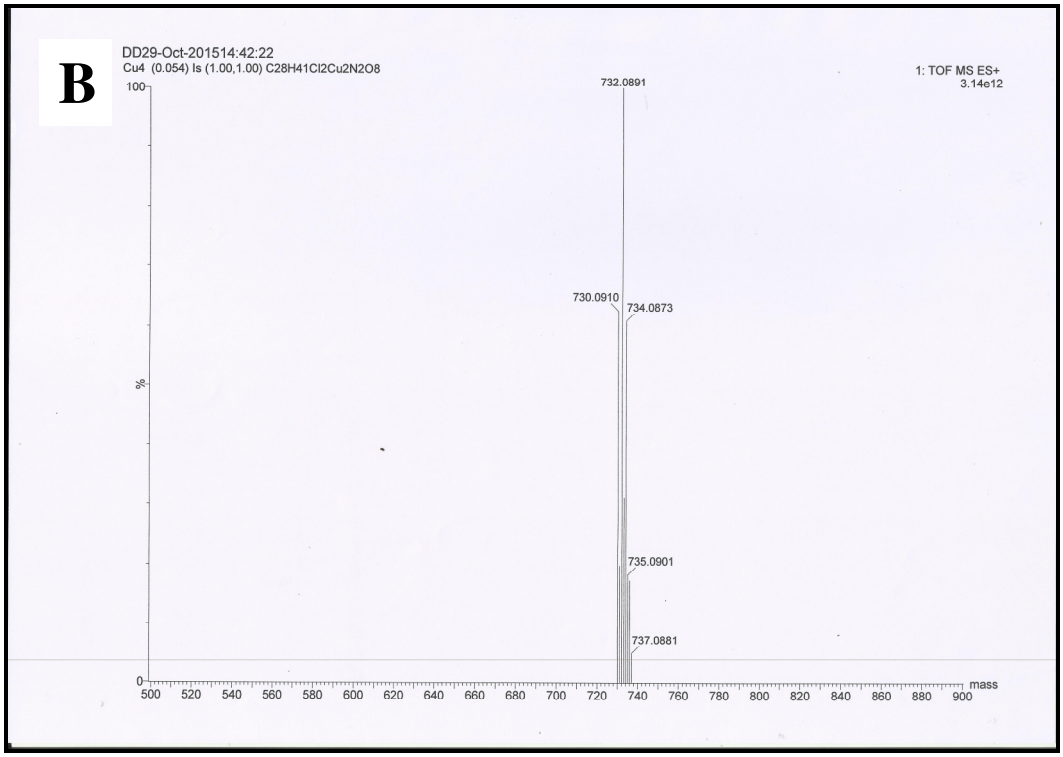

Fig. S26 ESI-MS spectrum of complex **4** in acetonitrile **(A)** experimental **(B)** simulated.

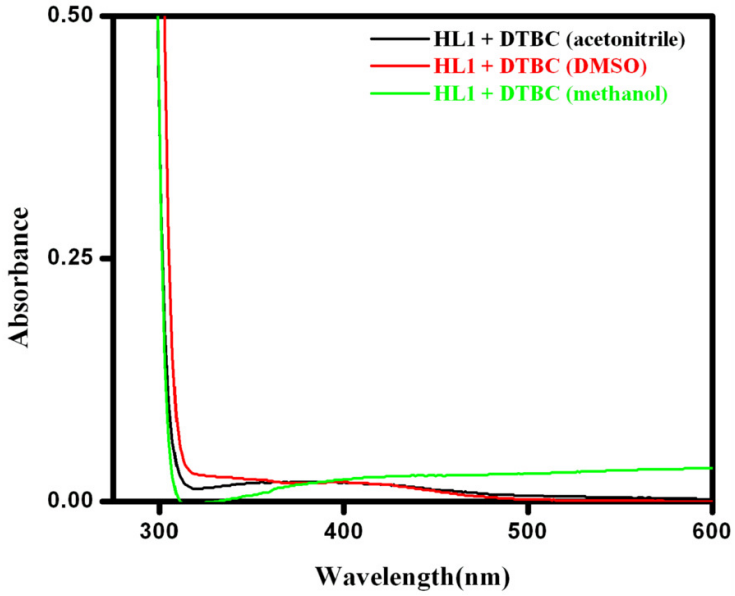

Fig. S27 Control experiment for catecholase activity with 3,5-DTBC and ligand HL1 in three solvents. Conditions: [3,5-DTBC]=10^{-2} (M); [HL1]=10^{-4} (M); Temperature=298 K; Total time after mixing= 1 hour.

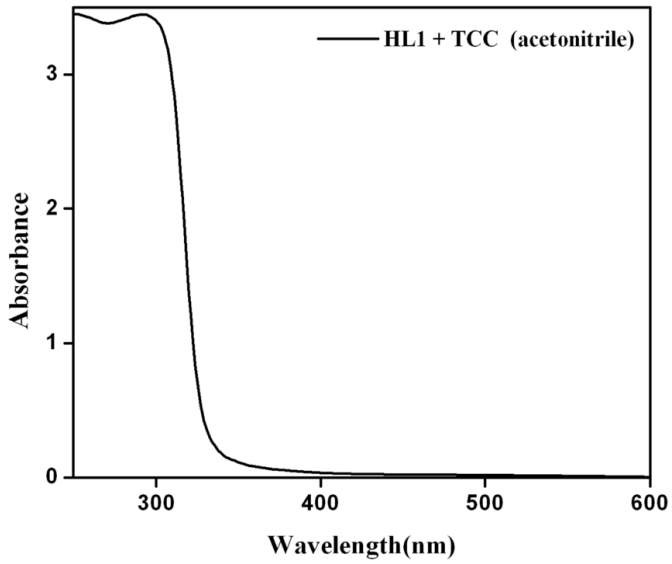

Fig. S28 Control experiment for catecholase activity with TCC and ligand HL1 in acetonitrile. Conditions: [TCC]=10^{-2} (M); [HL1]=10^{-4} (M); Temperature=298 K; Total time after mixing= 1 hour.

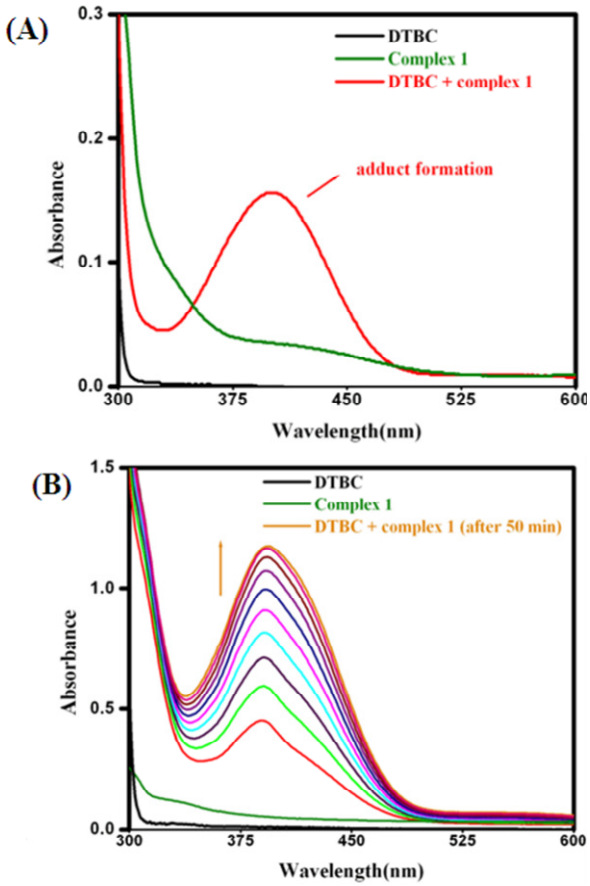

Fig. S29 UV-vis scan of a mixture of 3,5-DTBC and complex **1** (molar stoichiometry=100:1) in (**A**) acetonitrile and (**B**) methanol recorded for 50 min at an interval of 5 min.

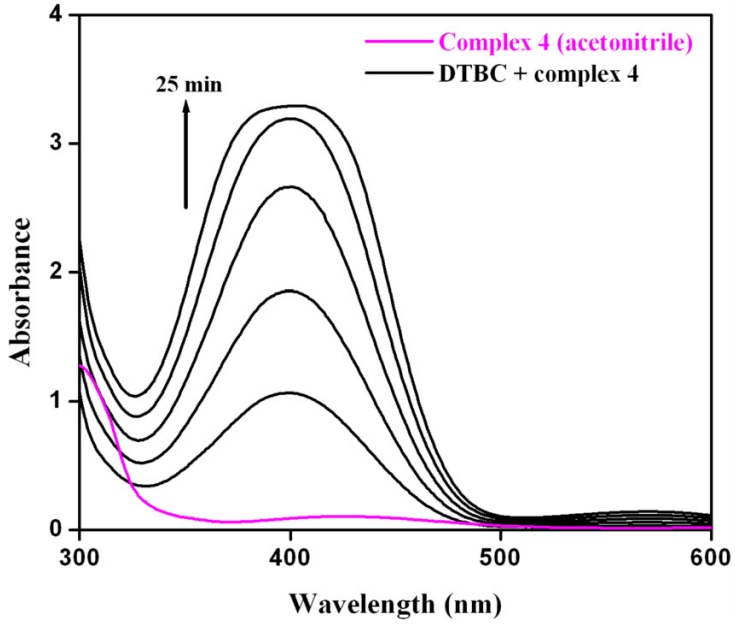

Fig. S30 Wavelength scan of a mixture of complex **4** and **3**,5-DTBC in 1:100 molar ratio in acetonitrile for 1 hour at an interval of 5 minutes. Conditions: [Complex **4**]=10^{-4} (M); [3,5-DTBC]=10^{-2} (M); Temperature=298K.

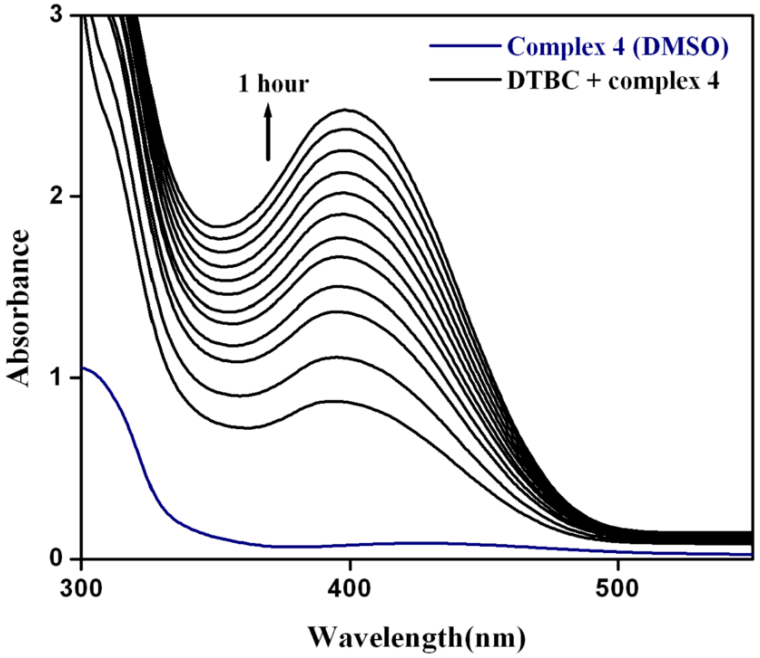

Fig. S31 Wavelength scan of a mixture of complex **4** and 3,5-DTBC in 1:100 molar ratio in DMSO for 1 hour at an interval of 5 minutes. Conditions: [Complex **4**]=10^{-4} (M); [3,5-DTBC]=10^{-2} (M); Temperature=298K.

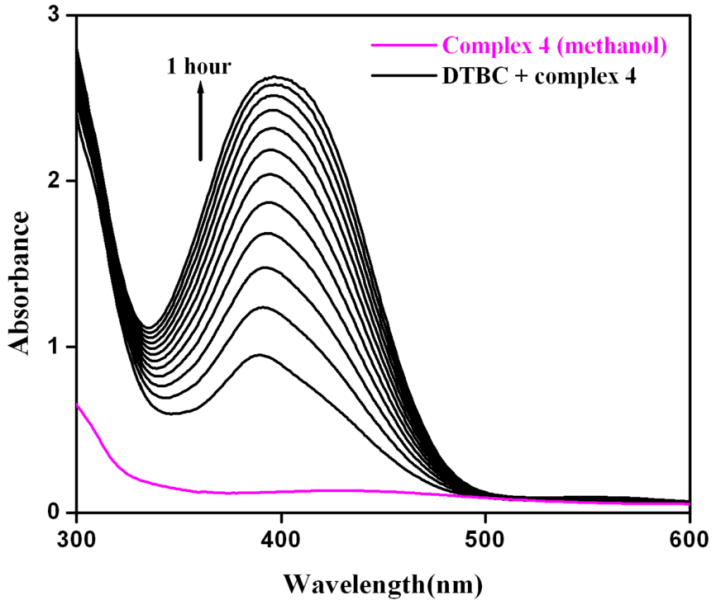

Fig. S32 Wavelength scan of a mixture of complex **4** and 3,5-DTBC in 1:100 molar ratio in methanol for 1 hour at an interval of 5 minutes. Conditions: [Complex **4**]=10^{-4} (M); [3,5-DTBC]=10^{-2} (M); Temperature=298K.

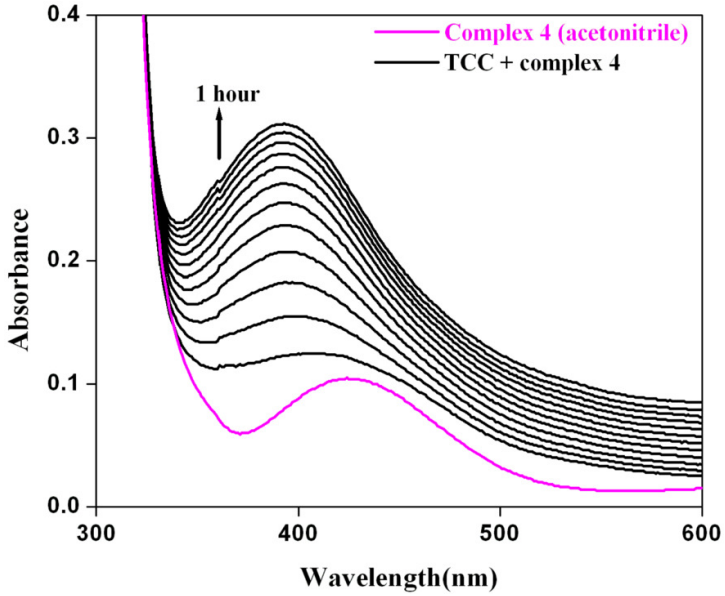

Fig. S33 Wavelength scan of a mixture of complex **4** and TCC in 1:100 molar ratio in acetonitrile for 1 hour at an interval of 5 minutes. Conditions: [Complex **4**]=10^{-4} (M); [TCC]=10^{-2} (M); Temperature=298K.

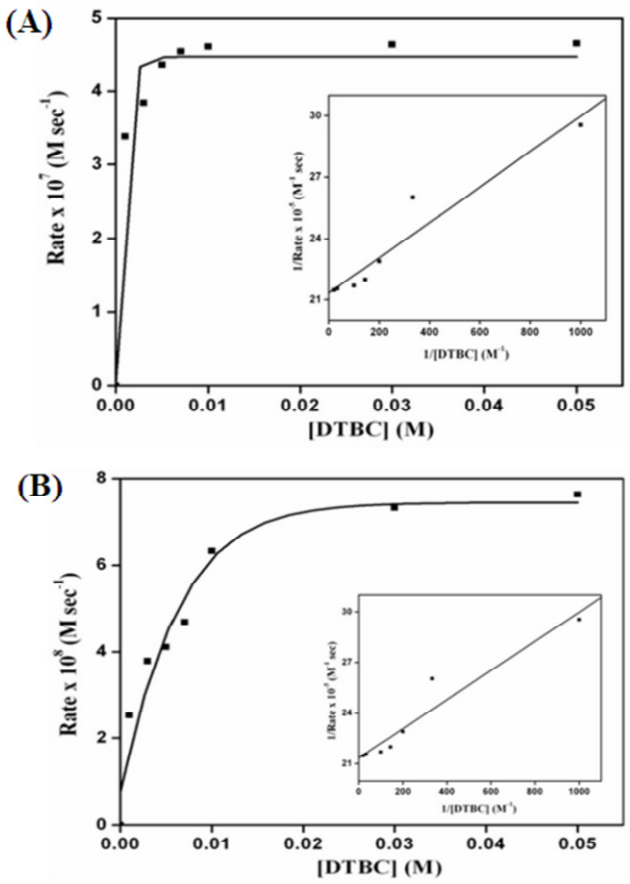

Fig. S34 Kinetic plot of rate vs [3,5-DTBC] (V vs S) for the catecholase activity of complex **1** in (A) methanol (R^2 = 0.963, Intercept=21.33417 and Error=0.4433, Slope=0.00865 and Error=0.00108) and (B) DMSO (R^2 = 0.954, Intercept=152.63328 and Error=15.01562, Slope=0.25931 and Error=0.03653) at 298 K. Inset shows the double-reciprocal plot (1/V vs 1/S) for the same.

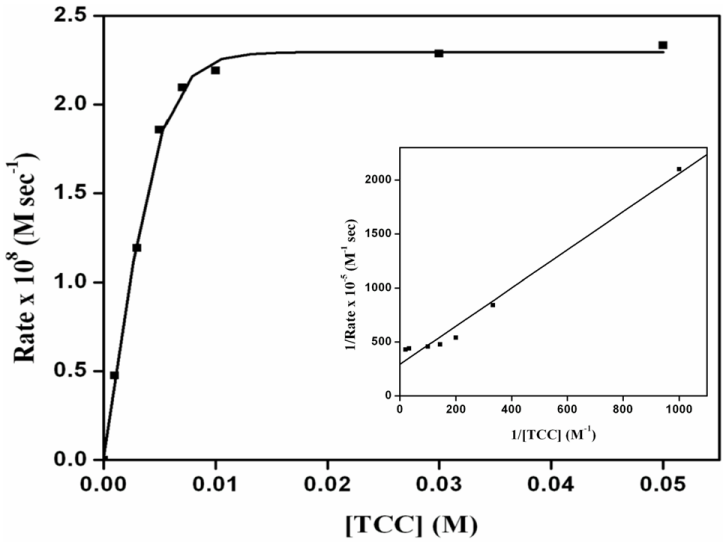

Fig. S35 Kinetic plot of rate vs [TCC] (V vs S) for the catecholase activity of complex **1** in acetonitrile at 298 K. Inset shows the double-reciprocal plot (1/V vs 1/S) for the same having R^2 = 0.992 (Intercept=292.35692and Error=42.2376, Slope=1.76649 and Error=0.10274).

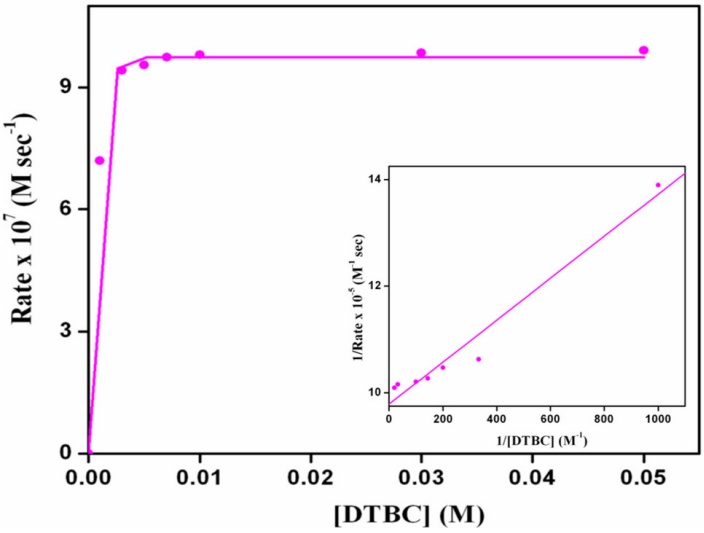

Fig. S36 Kinetic plot of rate vs [3,5-DTBC] (V vs S) for the catecholase activity of complex **4** in acetonitrile at 298 K. Inset shows the double-reciprocal plot (1/V vs 1/S) for the same having R^2=0.983 (Intercept=9.7875 and Error=0.1347, Slope=0.0039 and Error=3.279×10^{-4}).

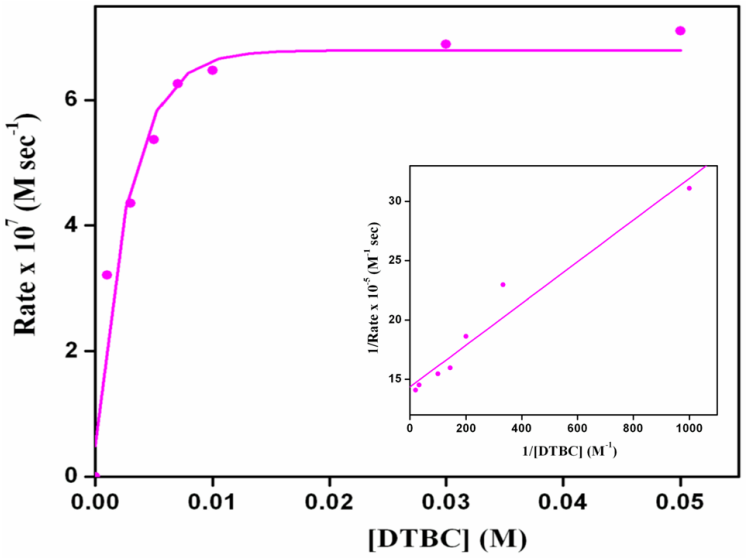

Fig. S37 Kinetic plot of rate vs [3,5-DTBC] (V vs S) for the catecholase activity of complex **4** in DMSO at 298 K. Inset shows the double-reciprocal plot (1/V vs 1/S) for the same having R^2=0.983 (Intercept=14.358 and Error=0.712, Slope=0.0176 and Error=0.0017).

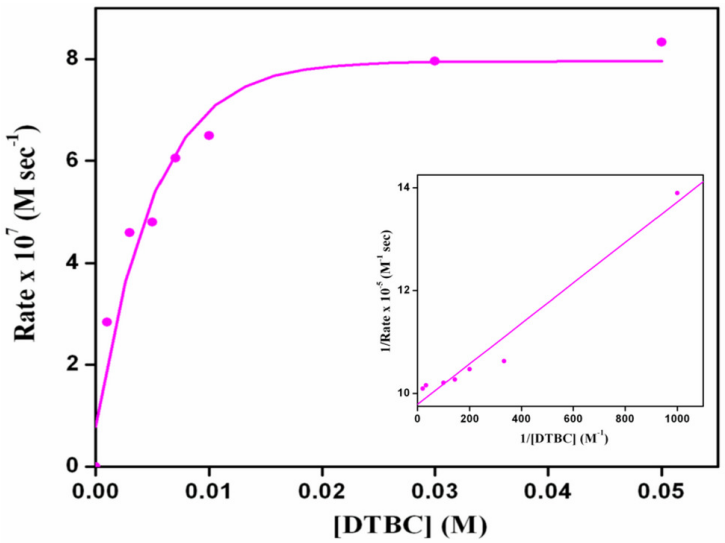

Fig. S38 Kinetic plot of rate vs [3,5-DTBC] (V vs S) for the catecholase activity of complex **4** in methanol at 298 K. Inset shows the double-reciprocal plot (1/V vs 1/S) for the same having R^2=0.983 (Intercept=9.7875 and Error=0.1348, Slope=0.0039 and Error=3.279×10^{-4}).

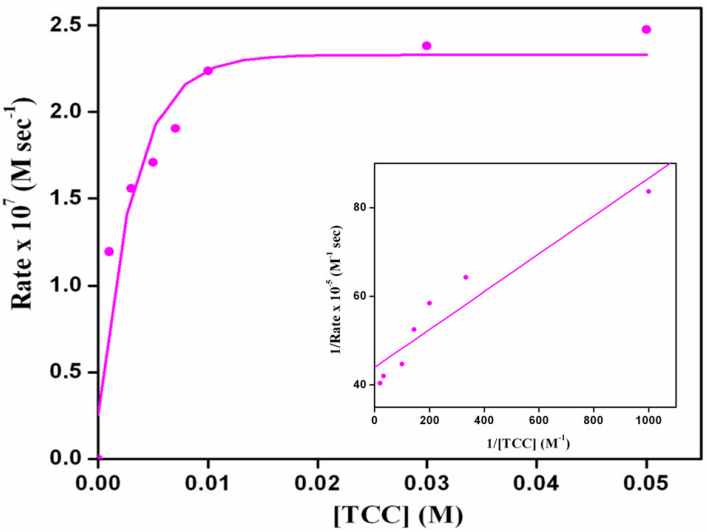

Fig. S39 Kinetic plot of rate vs [TCC] (V vs S) for the catecholase activity of complex **4** in acetonitrile at 298 K. Inset shows the double-reciprocal plot (1/V vs 1/S) for the same having R^2=0.953 (Intercept=43.983 and Error=2.505, Slope=0.043 and Error=0.006).

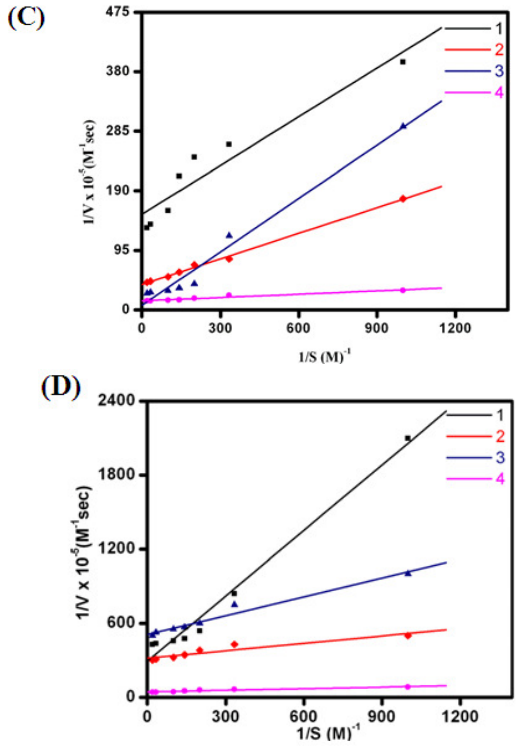

Fig. S40 Overlay of Line-weaver Burk plots for complexes **1-4** with 3,5-DTBC in DMSO (**C**) and with TCC in acetonitrile (**D**).

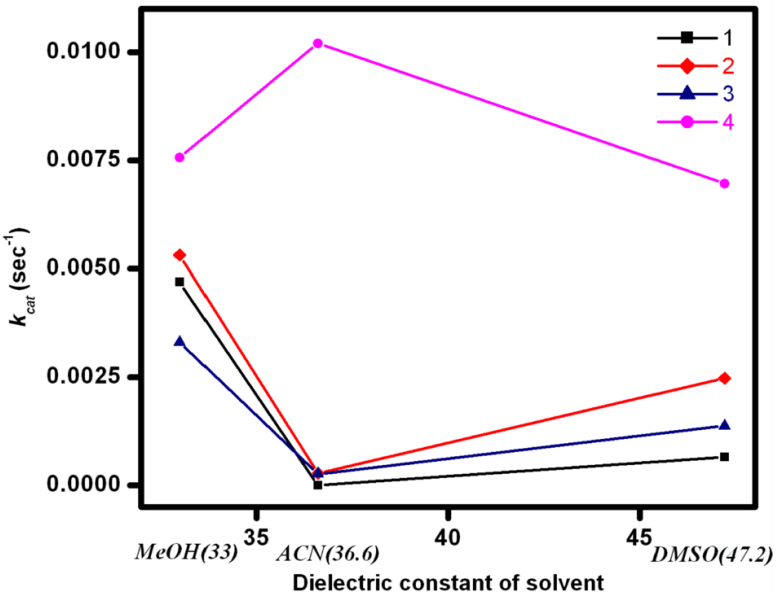

Fig. S41 Variation of k_{cat} values of complex **1-4** with dielectric constant of the solvents.

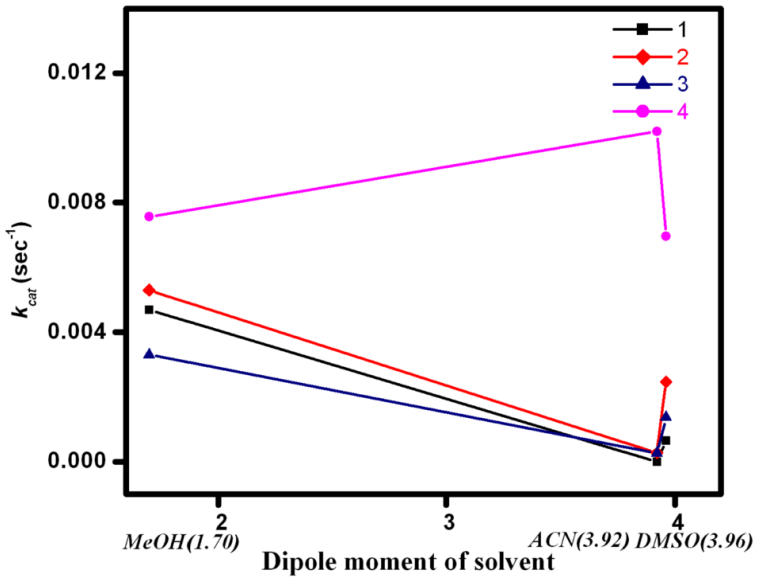

Fig. S42 Variation of k_{cat} values of complex **1-4** with dipole moment of the solvents.

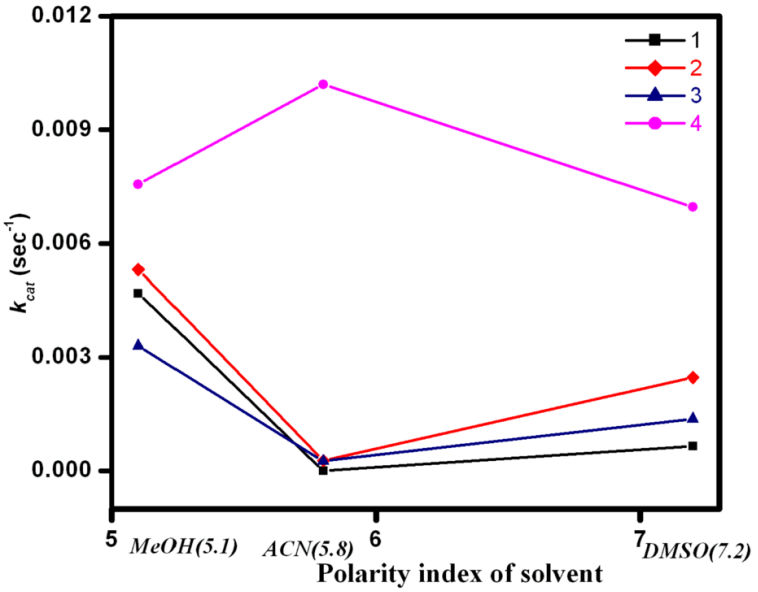

Fig. S43 Variation of k_{cat} values of complex **1 - 4** with polarity index of the solvents.

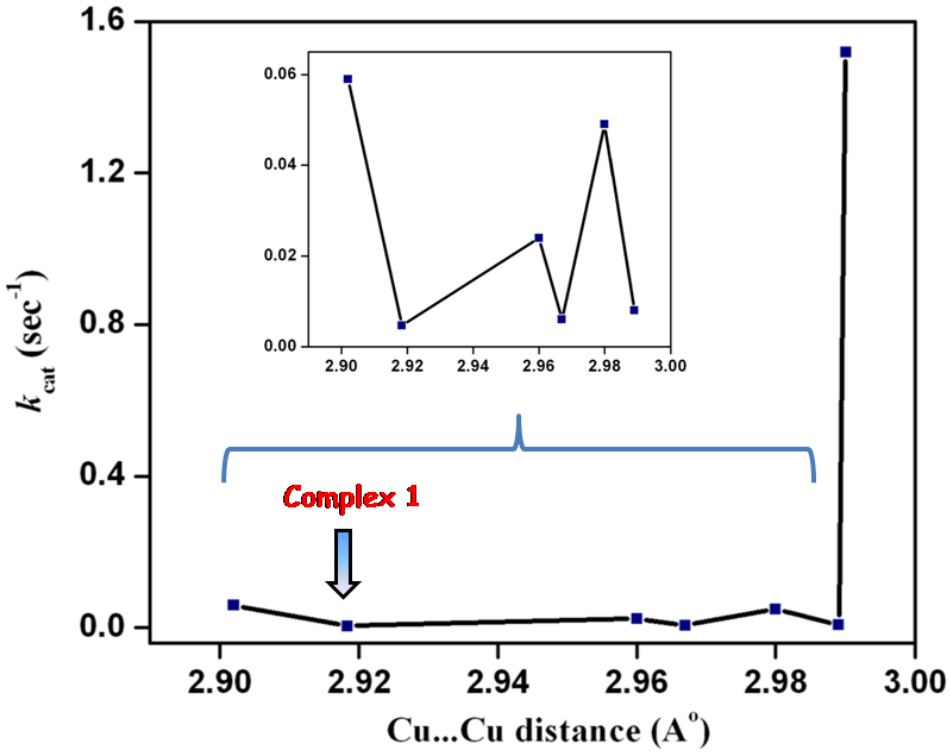

Fig. S44 Interdependence of intermetallic distance and catecholase activity in dinuclear Cu^{II} complex having both phenoxido and hydroxo bridge.

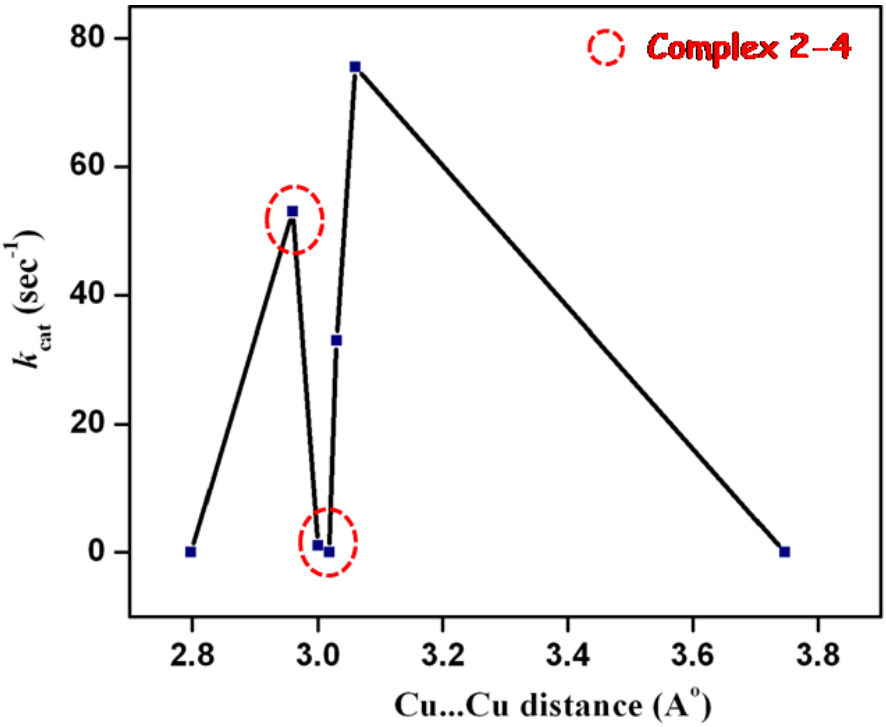

Fig. S45 Interdependence of intermetallic distance and catecholase activity in dinuclear Cu^{II} complex having only phenoxido bridge.

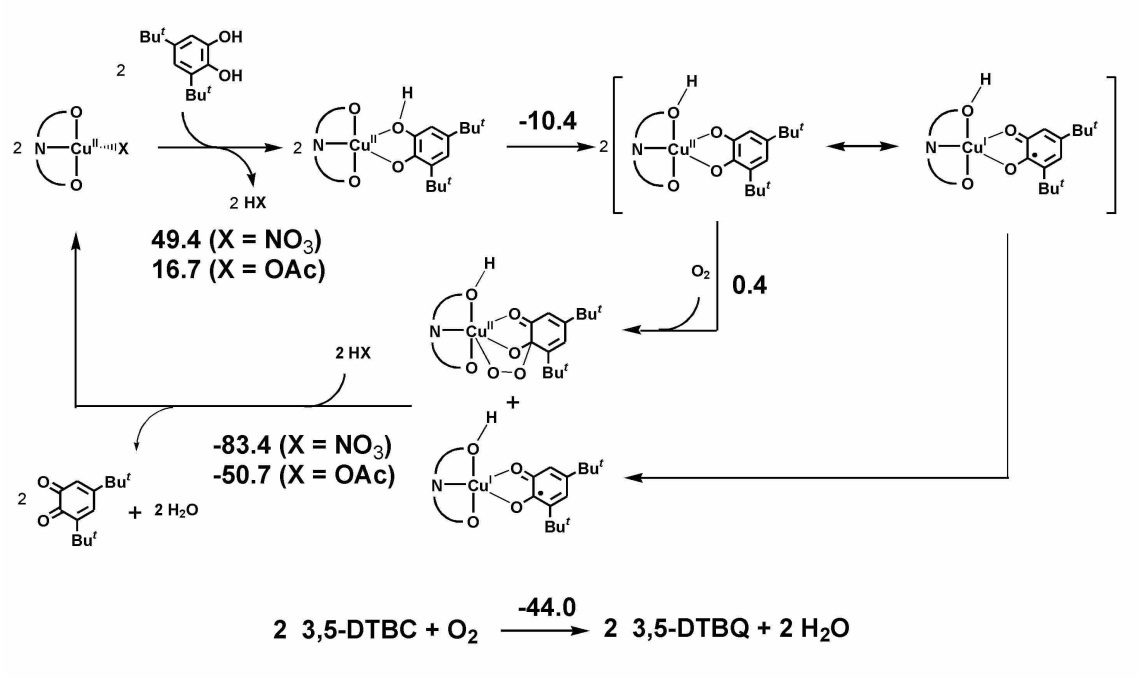

Fig. S46. B3LYP/DGDZVP energy changes (kcal mol^{-1}) in the catalytic cycle based on the monomeric neutral species derived from complexes **3** and **4** in MeCN solution.

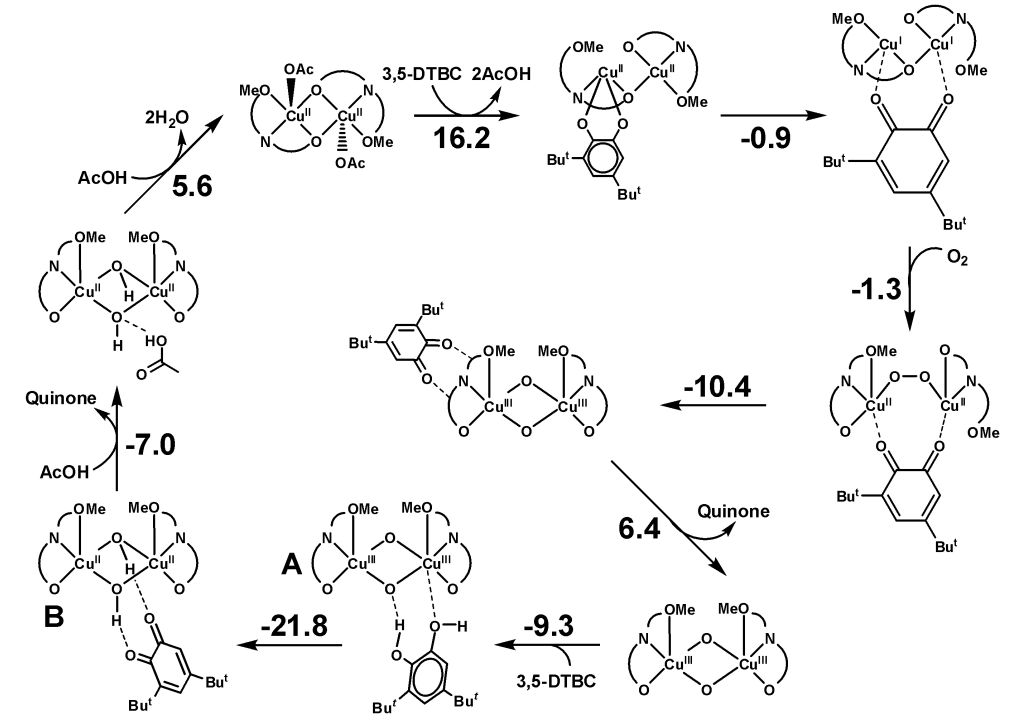

Fig. S47. PBE/TZ2P energy changes (kcal mol^{-1}) in the catalytic cycle based on complex **4** without coordination of AcOH on the complexes.

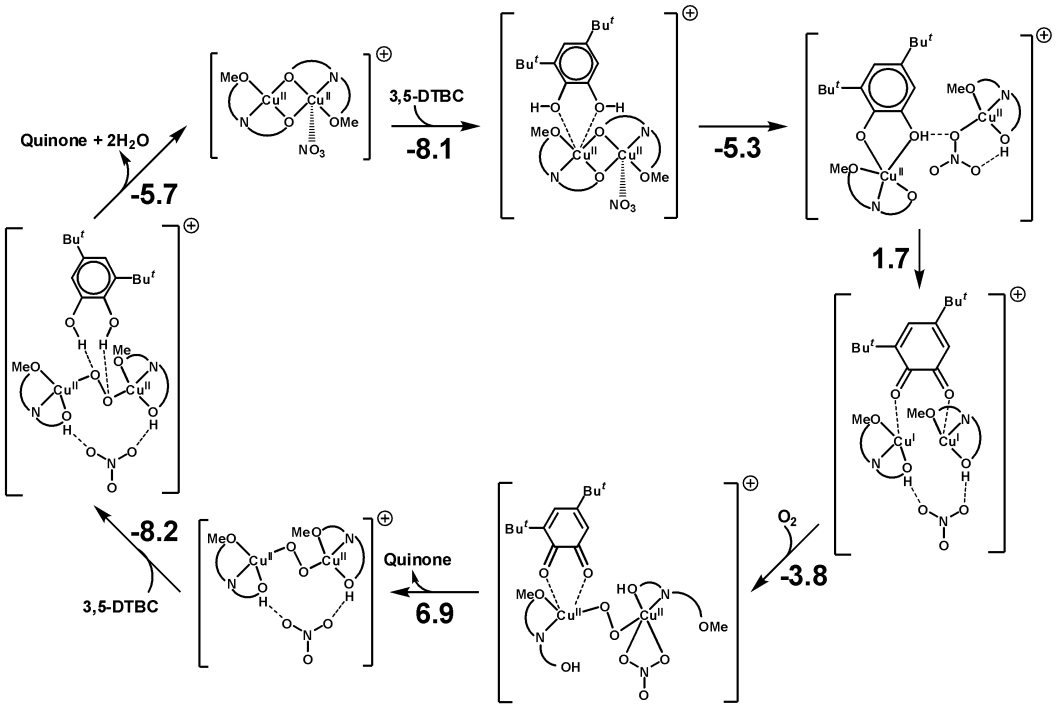

Fig. S48. Oxidation of 3,5-DTBC catalyzed by $[Cu_2(L2)_2(NO_3)]^+$. The energy changes (kcal/mol) estimated at the PBE/TZ2P level of theory for each step are given.

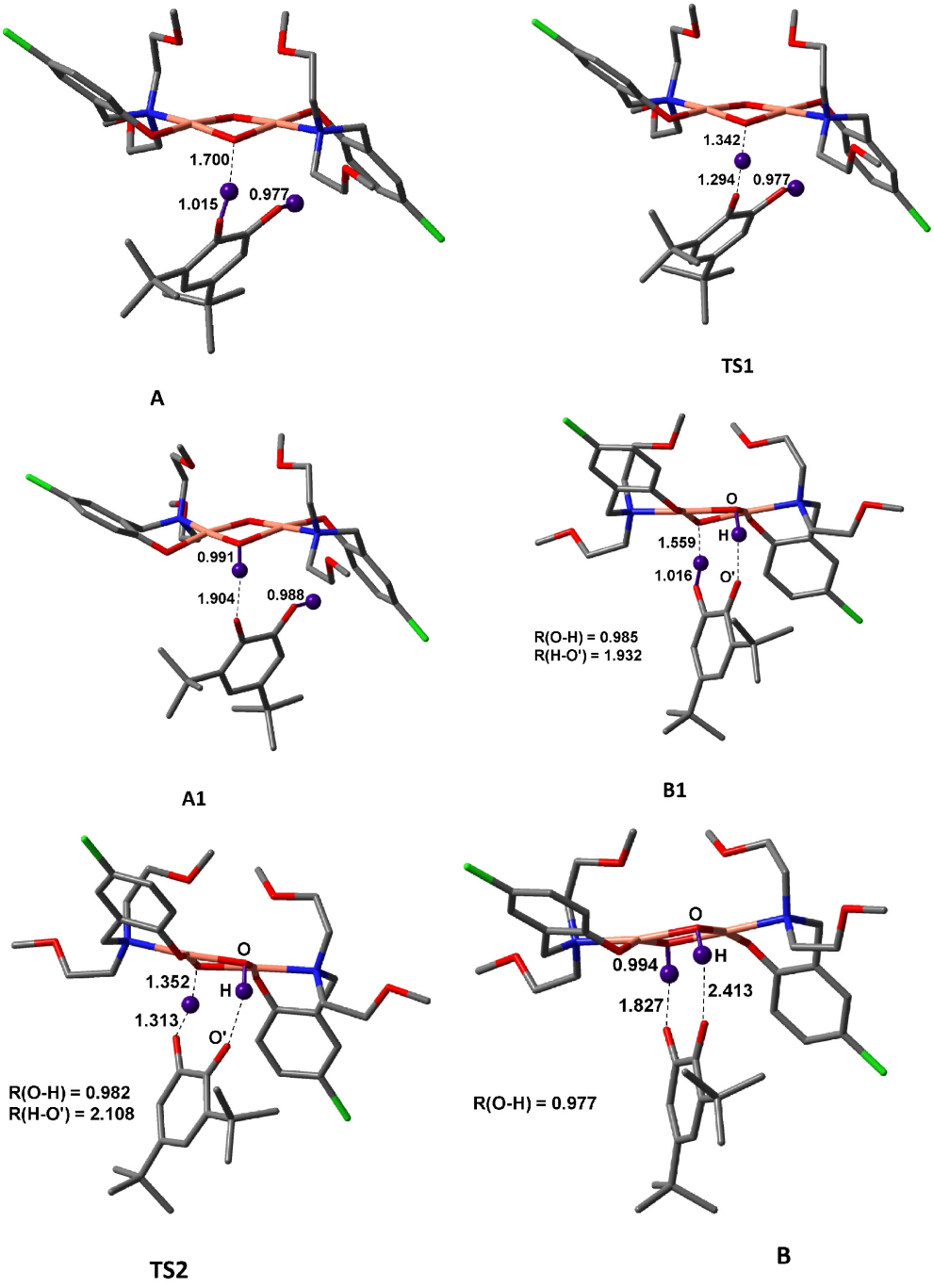

Fig. S49. Optimized (PBE/TZ2P) structures of the intermediates and transition states corresponding to the A→B reaction (Fig. 14). The O-H distances (Å) are given.

Table S1 Theoretical and experimental weight loss (from thermograms) of the complexes (End product = CuO).

Complex	**Final temperature**	**% weight loss**	
		Theoretical	**Experimental**
3	664°C	90.02	91.36
4	678°C	90.17	85.97

Table S2 Molar conductance values (Scm^2mol^{-1}) of copper complexes at 298 K.

Complex	**DMSO**		**Acetonitrile**		**Methanol**	
	Value	**Nature**	**Value**	**Nature**	**Value**	**Nature**
1	75	1:1	166	1:1	143	1:1
2	70	1:1	160	1:1	145	1:1
3	60	1:1	69	1:1	128	1:1
4	45	1:1	50	1:1	33	1:1

Table S3 Kinetic parameters for catecholase activity of complex **1**-**4** with 3,5-DTBC.

Complex	**Solvent**	V_{max} × 10^7 (s^{-1})	**Standard error** × 10^7 (s^{-1})	k_M × 10^7 (M)	**Standard error** × 10^9 (M)	k_{assoc} × 10^{-7} (M^{-1})	k_{cat}/k_M × 10^{-4} ($M^{-1}s^{-1}$)
1	Acetonitrile	-	-	-	-	-	-
	DMSO	0.65	0.065	0.17	4.06	5.88	3.86

	Methanol	4.69	0.1	405	0.59	2.47	0.01
2	Acetonitrile	0.27	0.01	0.14	1.88	7.14	1.95
	DMSO	2.47	0.07	0.34	1.94	2.94	7.35
	Methanol	5.31	0.30	0.18	2.00	5.55	29.17
3	Acetonitrile	0.26	0.09	1.13	48.6	0.88	0.23
	DMSO	1.37	0.85	0.39	0.26	2.56	3.52
	Methanol	3.41	0.10	0.21	1.35	4.76	16.55
4	Acetonitrile	10.20	0.11	0.04	0.38	25.00	250.00
	DMSO	6.96	0.38	0.12	1.89	8.33	57.00
	Methanol	7.56	0.22	0.17	23.03	5.88	43.9

Table S4 Kinetic parameters for catecholase activity of complex **1**-**4** with TCC in acetonitrile.

Complex	V_{max} × 10^7 (s^{-1})	**Standard error × 10^8**	k_M × 10^7 (M)	**Standard error × 10^8**	k_{assoc} × 10^{-7} (M^{-1})	k_{cat}/k_M × 10^{-4} ($M^{-1}s^{-1}$)
1	0.34	0.50	0.604	1.25	1.66	0.57
2	0.31	0.13	0.063	0.76	15.87	5.00
3	0.19	0.07	0.0998	0.11	10.02	1.96
4	2.27	1.24	0.097	0.19	10.31	23.45

Table S5 First-Order Rate Constants for the oxidation of 3,5-DTBC by Previously Reported Dinuclear Cu^{II} Complexes of Mannich-base and closely similar ligand systems[a]

Complex	Cu…Cu (Å)	Bridging	Solvent	k_{cat} (sec^{-1})	Reference
$[Cu_2(L^1\text{- O})(\mu\text{ -OH})][ClO_4]_2$, $[Cu_2(L^3\text{- O})(\mu\text{-}C_3H_3N_2)(OClO_3)(H_2O)][ClO_4]$. H_2O, $[Cu_2(L^4)(\mu\text{-OH})_2][ClO_4]_2.H_2O$.	2.99 3.37 -	μ-OPh-μ-OH μ-OR-μ-Pz μ-OH	Acetonitrile	1.52 0.029 0.028	14c
$[Cu_2L_2(H_2O)_x].yH_2O$ (x,y=0-2)	~3	μ-OPh	Methanol	0.055-1.055	6b
$[Cu_2L_2(ClO_4)_2]$ $[Cu_2L_2(OH)]ClO_4$	3.018 2.798	μ-OPh	Methanol	0.026 0.065	11a
$[Cu_2(L^1)(OH)(EtOH)(H_2O)][ClO_4]_2.H_2O$ $[Cu_2(L^5)(OMe)][ClO_4]_2.2MeOH$ $[Cu_2(L^6)(OMe)(MeOH)\text{-}(ClO_4)]ClO_4$ $[Cu_2(L^7)(OMe)(MeOH)(ClO_4)]ClO_4$	2.902 - 2.938 2.874	μ-OH-μ-OPh - μ-HOMe-μ-OPh μ-HOMe-μ-OPh	Methanol	0.059 0.009 0.013 0.012	4b
$[Cu_2(L^1)(\mu\text{-OAc})](ClO_4)_2\cdot(CH_3)_2CHOH$ $[Cu_2(L^2)\text{-}(\mu\text{-OAc})](ClO_4)\cdot H_2O\cdot(CH_3)_2CHOH$ $[Cu_2(L^3)(\mu\text{-OAc})]^{2+}$	3.3975 3.4837 -		Methanol-water (1:1); pH=8.5	0.025 0.051 0.0078	11c,24a
$[Cu_2(EBA)(H_2O)_4]^{4+}$	2.988	Double- μ-OH	Methanol-	0.05	9

			water(30:1),pH= 5.1		
$[Cu_2(L_{OCH3})(\mu\text{-OH})][(ClO_4)_2].C_4H_8O$, $[Cu_2(L_F)(\mu\text{-OH})][(ClO_4)_2]$	2.98 2.967	μ-OH-μ-OPh	Acetonitrile or Acetonitrile-water(20:80),pH =7	0.049 0.006	11b
$[Cu_2(LB5)(H_2O)_2][ClO_4]_4$ $[Cu_2(L\text{-}55)]^{4+}$	8.019 -	-	Methanol-water(30:1),pH= 5.1	0.035 0.33	10b
$[Cu_2(BPMP)(OH)][ClO_4]_2$ 0.5C4H8O	2.96	μ-OH-μ-OPh	Acetonitrile or Acetonitrile-water(20:80),pH =7	0.024	5b
$[Cu_2(H_2L)(\mu\text{-OH})](ClO_4)_2$, $[Cu_2(L)(H_2O)_2]PF_6$	2.9893 3.747	μ-OH-μ-OPh μ-OPh	Methanol-water(30:1),pH= 8.5	0.008 0.01	7a
$[Cu_2(H_2\text{-bbppnol})(\mu\text{-OAc})(H_2O)_2]Cl_2.2H_2O$ $[Cu_2(Hbtppnol)(\mu\text{-OAc})](ClO_4)_2$ $[Cu_2(P1\text{-}O^-)(OAc^-)]\text{-}(ClO_4)_2$	~3.40	μ-OAc	Methanol-water(30:1),pH= 8	0.0079 0.0078 0.0028	10c
$[Cu_2(L1)(\mu\text{-}OAc)_2](BF_4)\cdot 0.25Et_2O$ $[Cu_2(L2)(\mu\text{-}OAc)_2](BF4)$ $[Cu_2(L3)(\mu\text{-}OAc)_2](BF_4)\cdot 0.25MeOH\cdot 0.75H_2O$	3.304 3.263 3.299	μ-OAc-μ-OPh	Methanol	0.003 0.008 0.0001	16c

[a]OPh=phenoxido, Pz=pyrazolate.

Table S6. Selected interatomic distances (Å) in the optimized **3** and **4** molecules (triplet states). The atom notations correspond to those in Figs. 6, 7.

Atoms	Complex **3**		Complex **4**	
	PBE/TZ2P	B3LYP/DGDZVP	PBE/TZ2P	B3LYP/DGDZVP
Cu-O(1)	1.973	1.970	1.983	1.987
Cu-O(1')	2.067	2.044	2.058	2.037
Cu-O(3)	2.467	2.458	2.468	2.453
Cu-O(4)	1.983	1.993	1.970	1.964
Cu-N(1)	2.127	2.125	2.123	2.124
Cu-Cu'	3.085	3.071	3.094	3.091

Table S7. Energy changes in the reactions corresponding to oxidation of 3,5-DTBC catalyzed by $[Cu_2(L2)_2(AcO)_2]$ (Fig. 13).

Reaction	ΔE, kcal mol^{-1}
$[Cu^{II}_2(L2)_2(OAc)_2] + CatH_2 \rightarrow [Cu^{II}_2(L2)_2(Cat)]\cdot 2AcOH$	-0.4
$[Cu^{II}_2(L2)_2(Cat)]\cdot 2AcOH \rightarrow [Cu^{I}_2(L2)_2(3,5\text{-}DTBQ)]\cdot 2AcOH$	-0.9
$[Cu^{I}_2(L2)_2(3,5\text{-}DTBQ)]\cdot 2AcOH + O_2 \rightarrow [Cu^{II}_2(L2)_2(3,5\text{-}DTBQ)(O_2)]\cdot 2AcOH$	-1.3
$[Cu^{II}_2(L2)_2(3,5\text{-}DTBQ)(O_2)]\cdot 2AcOH \rightarrow [Cu^{III}_2(L2)_2(O_2)]\cdot(3,5\text{-}DTBQ)\cdot AcOH +$ + AcOH	-2.1
$[Cu^{III}_2(L2)_2(O_2)]\cdot(3,5\text{-}DTBQ)\cdot AcOH + AcOH \rightarrow [Cu^{III}_2(L2)_2(O_2)]\cdot 2AcOH +$ + 3,5-DTBQ	-1.9
$[Cu^{III}_2(L2)_2(O_2)]\cdot 2AcOH + CatH_2 \rightarrow [Cu^{III}_2(L2)_2(O_2)(CatH_2)]\cdot AcOH + AcOH$	-1.0
$[Cu^{III}_2(L2)_2(O_2)(CatH_2)]\cdot AcOH \rightarrow [Cu^{II}_2(L2)_2(OH)_2(3,5\text{-}DTBQ)] + AcOH$	-13.5
$[Cu^{II}_2(L2)_2(OH)_2(3,5\text{-}DTBQ)] + AcOH \rightarrow [Cu^{II}_2(L2)_2(OH)_2(AcOH)] + 3,5DTBQ$	-7.0
$[Cu^{II}_2(L2)_2(OH)_2(AcOH)] + AcOH \rightarrow [Cu^{II}_2(L2)_2(OAc)_2] + 2H_2O$	5.6

Table S8. Energy changes in the reactions corresponding to oxidation of 3,5-DTBC catalyzed by monomeric copper complexes (Fig S46).

Reaction	ΔE, kcal mol^{-1}
$2[Cu^{II}(L2)(NO_3)] + 2CatH_2 \rightarrow 2[Cu^{II}(L2)(CatH)] + 2HNO_3$	49.4
$2[Cu^{II}(L2)(OAc)] + 2CatH_2 \rightarrow 2[Cu^{II}(L2)(CatH)] + 2AcOH$	16.7
$2[Cu^{II}(L2)(CatH)] \rightarrow 2\{[Cu^{II}(HL2)(Cat)] \leftrightarrow [Cu^{I}(HL2)(SQ)]\}$	-10.4
$\{[Cu^{II}(HL2)(Cat)] \leftrightarrow [Cu^{I}(HL2)(SQ)]\} + O_2 \rightarrow [Cu^{II}(HL2)(SQ)(O_2)]$	0.4
$[Cu^{II}(HL2)(SQ)(O_2)] + [Cu^{I}(HL2)(SQ)] + 2HNO_3 \rightarrow 2[Cu^{II}(L2)(NO_3)] + + 2(3,5\text{-DTBQ}) + 2H_2O$	-83.4
$[Cu^{II}(HL2)(SQ)(O_2)] + [Cu^{I}(HL2)(SQ)] + 2AcOH \rightarrow 2[Cu^{II}(L2)(OAc)] + + 2(3,5\text{-DTBQ}) + 2H_2O$	-50.7

Table S9. Energy changes in the reactions corresponding to the catalytic cycle based on complex **4** without coordination of AcOH on the complexes (Fig. S47).

Reaction	ΔE, kcal mol^{-1}
$[Cu^{II}_2(L2)_2(OAc)_2] + CatH_2 \rightarrow [Cu^{II}_2(L2)_2(Cat)] + 2AcOH$	16.2
$[Cu^{II}_2(L2)_2(Cat)] \rightarrow [Cu^{I}_2(L2)_2(3,5\text{-DTBQ})]$	-0.9
$[Cu^{I}_2(L2)_2(3,5\text{-DTBQ})] + O_2 \rightarrow [Cu^{II}_2(L2)_2(3,5\text{-DTBQ})(O_2)]$	-1.3
$[Cu^{II}_2(L2)_2(3,5\text{-DTBQ})(O_2)] \rightarrow [Cu^{III}_2(L2)_2(O_2)]\cdot(3,5\text{-DTBQ})$	-10.4
$[Cu^{III}_2(L2)_2(O_2)]\cdot(3,5\text{-DTBQ}) \rightarrow [Cu^{III}_2(L2)_2(O_2)] + 3,5\text{-DTBQ}$	6.4
$[Cu^{III}_2(L2)_2(O_2)] + CatH_2 \rightarrow [Cu^{III}_2(L2)_2(O_2)(CatH_2)]$	-9.3
$[Cu^{III}_2(L2)_2(O_2)(CatH_2)] \rightarrow [Cu^{II}_2(L2)_2(OH)_2(3,5\text{-DTBQ})]$	-21.8
$[Cu^{II}_2(L2)_2(OH)_2(3,5\text{-DTBQ})] + AcOH \rightarrow [Cu^{II}_2(L2)_2(OH)_2(AcOH)] + 3,5\text{DTBQ}$	-7.0
$[Cu^{II}_2(L2)_2(OH)_2(AcOH)] + AcOH \rightarrow [Cu^{II}_2(L2)_2(OAc)_2] + 2H_2O$	5.6

Table S10. Energy changes in the reactions corresponding to the oxidation of 3,5-DTBC catalyzed by $[Cu_2(L2)_2(NO_3)]^+$. (Fig. S8).

Reaction	ΔE, kcal mol^{-1}
$[Cu^{II}_2(L2)_2(NO_3)]^+ + CatH_2 \rightarrow [Cu^{II}_2(L2)_2(NO_3)(CatH_2)]^+$	-8.1
$[Cu^{II}_2(L2)_2(NO_3)(CatH_2)]^+ \rightarrow [Cu^{II}_2(L2)(HL2)(NO_3)(CatH)]^+$	-5.3
$[Cu^{II}_2(L2)(HL2)(NO_3)(CatH)]^+ \rightarrow [Cu^{I}_2(HL2)_2(NO_3)(3,5\text{-}DTBQ)]^+$	1.7
$[Cu^{I}_2(HL2)_2(NO_3)(3,5\text{-}DTBQ)]^+ + O_2 \rightarrow [Cu^{II}_2(HL2)_2(NO_3)(3,5\text{-}DTBQ)(O_2)]^+$	-3.8
$[Cu^{II}_2(HL2)_2(NO_3)(3,5\text{-}DTBQ)(O_2)]^+ \rightarrow [Cu^{II}_2(HL2)_2(NO_3)(O_2)]^+ + 3,5\text{-}DTBQ$	6.9
$[Cu^{II}_2(HL2)_2(NO_3)(O_2)]^+ + CatH_2 \rightarrow [Cu^{II}_2(HL2)_2(NO_3)(O_2)(CatH_2)]^+$	-8.2
$[Cu^{II}_2(HL2)_2(NO_3)(O_2)(CatH_2)]^+ \rightarrow [Cu^{II}_2(L2)_2(NO_3)]^+ + 3,5\text{-}DTBQ + 2H_2O$	-5.7